EurJIC
European Journal of Inorganic Chemistry

ChemPubSoc Europe

DOI:10.1002/ejic.201201428

Allyl-End-Grafted Carbosilane Dendrimers Based on 1,4-Phenylene Units: Synthesis, Reactivity, Structure, and Bonding Motifs

Zakariyya Ishtaiwi,[a] Tobias Rüffer,[a] Alexander Hildebrandt,[a] Firas F. Awwadi,[b] Harald Hahn,[a] Akerke Abylaikhan,[a] Deeb Taher,[b] Uwe Siegert,[a] Bernhard Walfort,[a] and Heinrich Lang*[a]

Dedicated to Professor Dr. Jaroslav Holeček on the occasion of his 80th birthday[‡]

Keywords: Dendrimers / Self-assembly / Supramolecular chemistry / Pi interactions / NMR spectroscopy

The synthesis of a series of carbosilanes of type 1-Br–C_6H_4–4-$SiMe_{3-n}(CH_2CH=CH_2)_n$ (n = 1, 2, 3), Si[C_6H_4–4-$SiMe_{3-n}(CH_2CH=CH_2)_n]_4$, 1-Br–$C_6H_4$-4-Si[$C_6H_4$–4-$SiMe_{3-n}$-$(CH_2CH=CH_2)_n]_3$ (n = 0, 1, 2, 3), ClSi[C_6H_4–4-Si{C_6H_4–4-$SiMe_{3-n}(CH_2CH=CH_2)_n\}_3]_3$, Si[$C_6H_4$–4-Si{$C_6H_4$–4-$SiMe_{3-n}$-$(CH_2CH=CH_2)_n\}_3]_4$ (n = 1, 2), and 1-Br–C_6H_4–4-Si[C_6H_4–4-Si{C_6H_4–4-$SiMe_{3-n}(CH_2CH=CH_2)_n\}_3]_3$ (n = 0, 1, 2, 3) is discussed. The structures of Si[C_6H_4–4-$SiMe_2(CH_2CH=CH_2)]_4$ (**7b**) and ClSi[C_6H_4–4-Si{C_6H_4–4-$SiMe_2(CH_2CH=CH_2)\}_3]_3$ (**10a**) in the solid state are reported. The crystal structures of both dendrimers are based on C–H···π_{CC} (π_{CC} = double bond of the $CH=CH_2$ groups) and π–π interactions. The 3D network structure observed for **7b** is composed of three crystallographically independent head-to-head stacking columns along the crystallographic b axis with π–π contacts among the C_6H_4 groups of neighboring molecules, with the columns interacting further by C–H···π_{CC} arrangements. Two molecules of **10a** interdigitate in the solid state to form self-complementary dimers that are stabilized by C–H···π_{CC} and π–π contacts. The structures of the monomer and the dimer were optimized by using the MM$^+$ force field as implemented in HyperChem 4.0^2. In addition, the presence of self-complementary structures in solution is evidenced from ^1H NMR spectroscopy. In dichloromethane solely dimeric species exist, whereas in benzene monomers are observed. Calculated electrostatic potentials were used to rationalize the supramolecular structures of these two carbosilane compounds.

Introduction

In general, dendrimers are three-dimensional, repetitively branched molecules with a high degree of molecular uniformity, narrow molecular-weight distribution, and they show specific size and shape characteristics. They can be prepared by the divergent, convergent, or a combination of these two synthetic methodologies to give highly functionalized macromolecules that feature end-grafted and internal functional groups.[1] Recent developments in this field of chemistry have been focused on different applications.[2–7] Depending on the nature of the dendrimer framework and the functional groups present at the dendrimer core, shell, or periphery, these molecules can be used as active components in the field of homogeneous and heterogeneous catalysis,[3] as liquid-crystalline materials,[4] as drug-delivery vehicles,[5] as ionophores for chemical sensing in sensor technology,[6] as tectons for self-assembly with network formation,[7a] and as nonlinear optical materials.[7b] In addition, dendrimers have found use in the synthesis and stabilization of mainly monodisperse metallic nanoparticles.[7c] Among them, much attention has been paid to the family of silicon-containing dendrimers including silanes, carbosilanes, siloxanes, carbosiloxanes, and silsesquioxanes.[8–13] The flexibility of aliphatic spacer units [$(CH_2)_n$; n = 2, 3] between the silicon branching points, however, produces some limitation in their application. Thus, in appropriate end-grafted palladium-, platinum-, rhodium-, or ruthenium-supported metallodendrimers not all the catalytic active centers are

---

[a] Department of Inorganic Chemistry,
Faculty of Natural Sciences, Institute of Chemistry,
Chemnitz University of Technology,
Strasse der Nationen 62, 09111 Chemnitz, Germany
Fax: +49-371-531-21219
E-mail: heinrich.lang@chemie.tu-chemnitz.de
Homepage: https://www.tu-chemnitz.de/chemie/anorg/
[b] Department of Chemistry,
The University of Jordan,
Amman 11942, Jordan

[‡] For his contribution to the chemistry of coordination and organometallic compounds.

Supporting information for this article is available on the WWW under http://dx.doi.org/10.1002/ejic.201201428.

accessible for the substrates. For this reason it is of interest to synthesize shape-persistent carbosilane dendrimers by using rigid spacer units between the silicon atoms.

In this report, we focus on the convergent synthesis of shape-persistent dendritic molecules with 1,4-phenylene spacer units.

Results and Discussion

A series of carbosilane dendrimers based on 1,4-substituted phenylene units is accessible in a consecutive synthesis procedure by using the convergent growth method including halide/lithium and lithium/silicon exchange reactions. The synthesis of the key starting materials 1-Br–C_6H_4–4-Si-$Me_{3-n}Cl_n$ (**3a**,[14] n = 0; **3b**,[15] n = 1; **3c**,[15] n = 2; **3d**,[16] n = 3) and 1-Br–C_6H_4–4-Si$Me_{3-n}(CH_2CH{=}CH_2)_n$ (**5a**,[17] n = 1; **5b**, n = 2; **5c**,[18] n = 3) is depicted in Scheme 1. As a suitable precursor, 1,4-dibromobenzene was used, which was either monolithiated (synthesis of **3a**) or transformed into bromophenylmagnesium bromide (synthesis of **3b**–**3d**) and subsequently treated with the chlorosilanes Si$Me_{3-n}Cl_{n+1}$ (**2a**, n = 0; **2b**, n = 1; **2c**, n = 2; **2d**, n = 3) to obtain compounds **3a**–**3d**. Treatment of **3b**–**3d** with allylmagnesium bromide gave **5a**–**5c**. After appropriate workup, carbosilanes **3a**–**3d** and **5a**–**5c** could be isolated as colorless liquids that dissolve in most common organic solvents.

The zeroth-generation dendrimers Si[C_6H_4–4-SiMe_{3-n}-$(CH_2CH{=}CH_2)_n$]$_4$ (**7b**,[19] n = 1; **7c**, n = 2; **7d**,[19] n = 3) were prepared similarly to Si(C_6H_4–4-SiMe_3)$_4$ (**7a**)[20] by lithiation of **5a**–**5c** followed by addition of SiCl_4 as depicted in Scheme 1. The yield of isolated **7b**–**7d** is 30–40% (see the Experimental Section). When 1-Br–C_6H_4–4-SiCl_3 (**3d**) is used instead of SiCl_4 then 1-Br–C_6H_4–4-Si[C_6H_4–4-SiMe_{3-n}-$(CH_2CH{=}CH_2)_n$]$_3$ (**8a**, n = 0; **8b**, n = 1; **8c**, n = 2; **8d**, n = 3) was obtained (yield 40–70%; Scheme 1; see the Experimental Section). Carbosilanes **7b**–**7d** and **8a**–**8d** are colorless solids that are soluble in most common organic solvents.

The first-generation dendrimers Si[C_6H_4–4-Si{C_6H_4–4-Si$Me_{3-n}(CH_2CH{=}CH_2)_n$}$_3$]$_4$ (**11a**, n = 1; **11b**, n = 2) are accessible by subsequent treatment of **8b** and **8c** with *t*BuLi and SiCl_4/TMEDA (TMEDA = *N*,*N*,*N*′,*N*′-tetramethylethylenediamine; Scheme 2; see the Experimental Section), in which TMEDA permits control of the selective formation of **11a** and **11b**. Without TMEDA, only the chlorocarbosilanes **10a** and **10b** formed. This confirms the higher nucleophilicity of the lithiated species **9a** and **9b** in the presence of TMEDA.[21]

As a starting material for the convergent synthesis of second-generation dendrimers, the availability of first-generation dendrons 1-Br–C_6H_4–4-Si[C_6H_4–Si{C_6H_4–4-SiMe_{3-n}-$(CH_2CH{=}CH_2)_n$}$_3$]$_3$ (**12a**, n = 0; **12b**, n = 1; **12c**, n = 2; **12d**, n = 3) is required. These carbosilanes can be synthesized from **8a**–**8d** in a two-step synthesis procedure including metalation of **8a**–**8d** with *t*BuLi followed by addition of 1-Br–C_6H_4–4-SiCl_3 (**3d**) [Equation (1)]. However, all attempts to synthesize **12a** failed due to insolubility of the intermediate products. In contrast, **12b**, **12c**, and **12d** are accessible by using diethyl ether/tetrahydrofuran mixtures of ratio 1:3 (v/v). After appropriate workup, **12b**–**12d** can be isolated as colorless solids in a yield between 8 and 25% (see the Experimental Section).

All compounds were fully characterized by elemental analysis as well as IR, ^1H, $^{13}C\{^1H\}$, and $^{29}Si\{^1H\}$ NMR spectroscopy. ESI-TOF mass spectrometry was additionally used to characterize **7c** and **8a**–**8d**, whereas MALDI-TOF studies were performed with **10a**, **11a**, and **12b**, respectively. The identities of **7b** and **10a** in the solid state were confirmed by single-crystal X-ray diffraction studies.

Single crystals of **7b** could be obtained by cooling a solution of **7b** in *n*-pentane to –30 °C. Compound **7b** crystallizes in the non-centrosymmetric chiral monoclinic space group $I2$. The asymmetric unit comprises two molecules of **7b** that

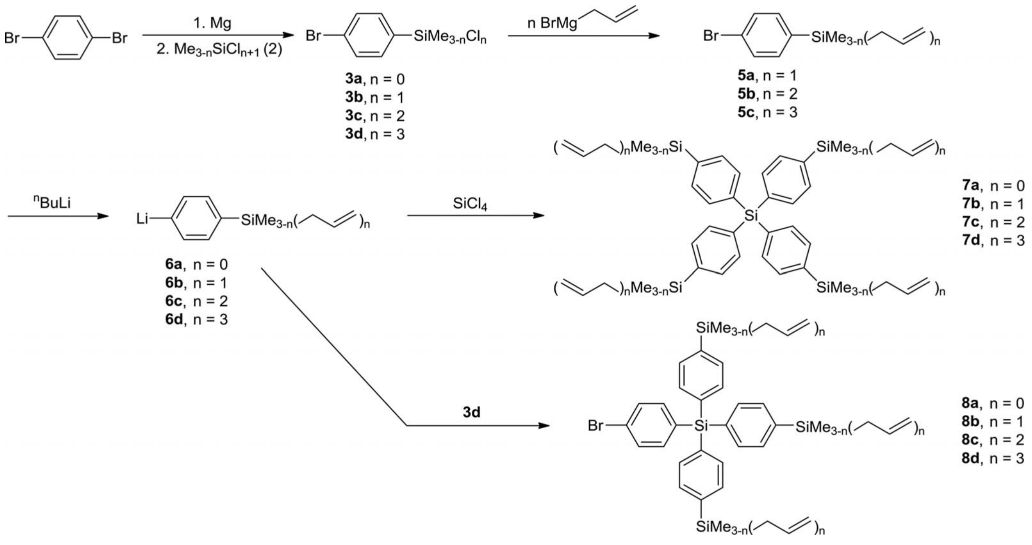

Scheme 1. Synthesis of **3a**–**3d**, **5a**–**5c**, **7a**–**7d**, and **8a**–**8d**.

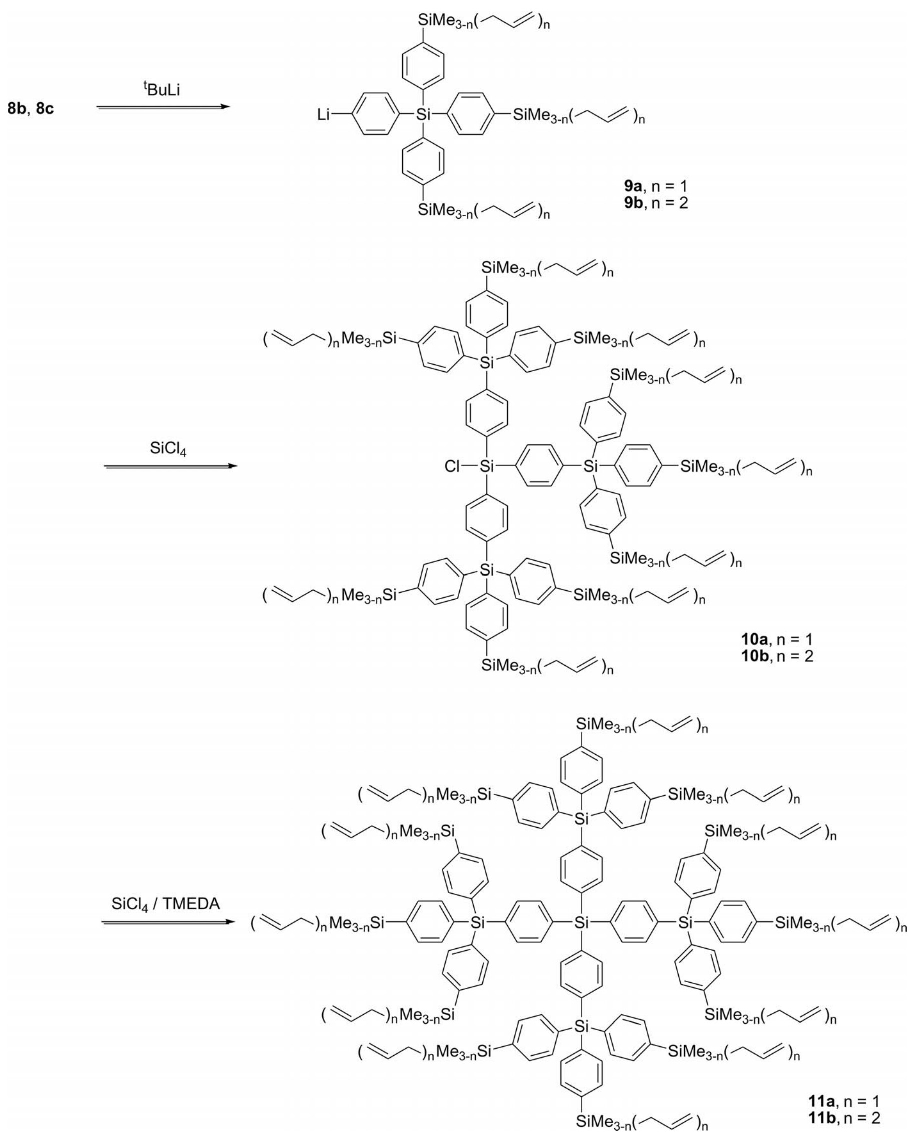

Scheme 2. Synthesis of dendrimers **10a**, **10b**, **11a**, and **11b**.

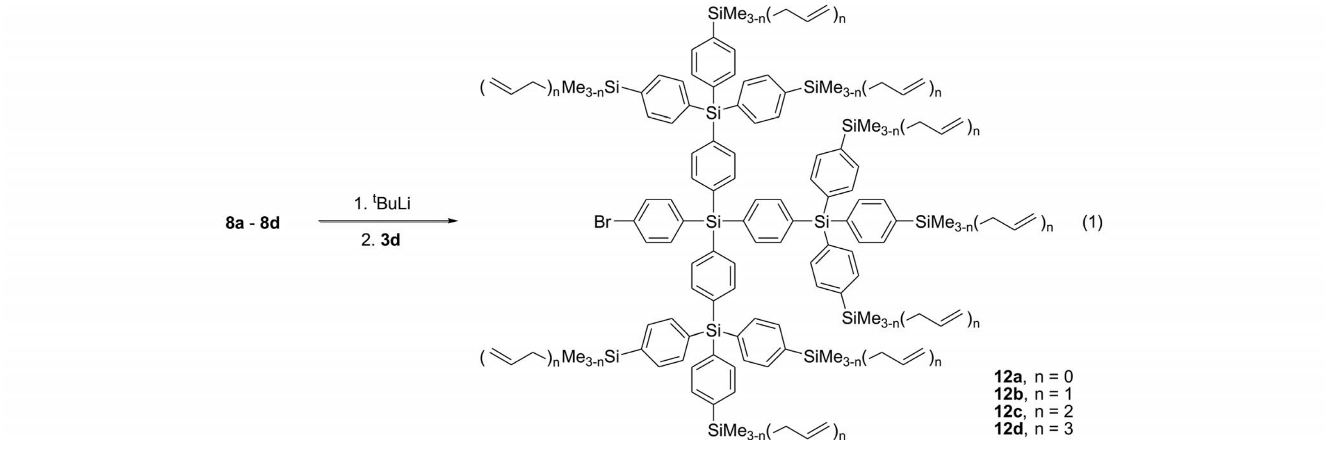

possess C_1 symmetry (**7b-I**, **7b-II**) and half of a further molecule that possesses crystallographically imposed C_2 symmetry (**7b-III**). The molecular structures of the three crystallographically independent molecules of **7b** (**7b-I**, **7b-II**, **7b-III**) as well as a packing diagram are illustrated in Figure 1. The crystal data and structure-refinement parameters

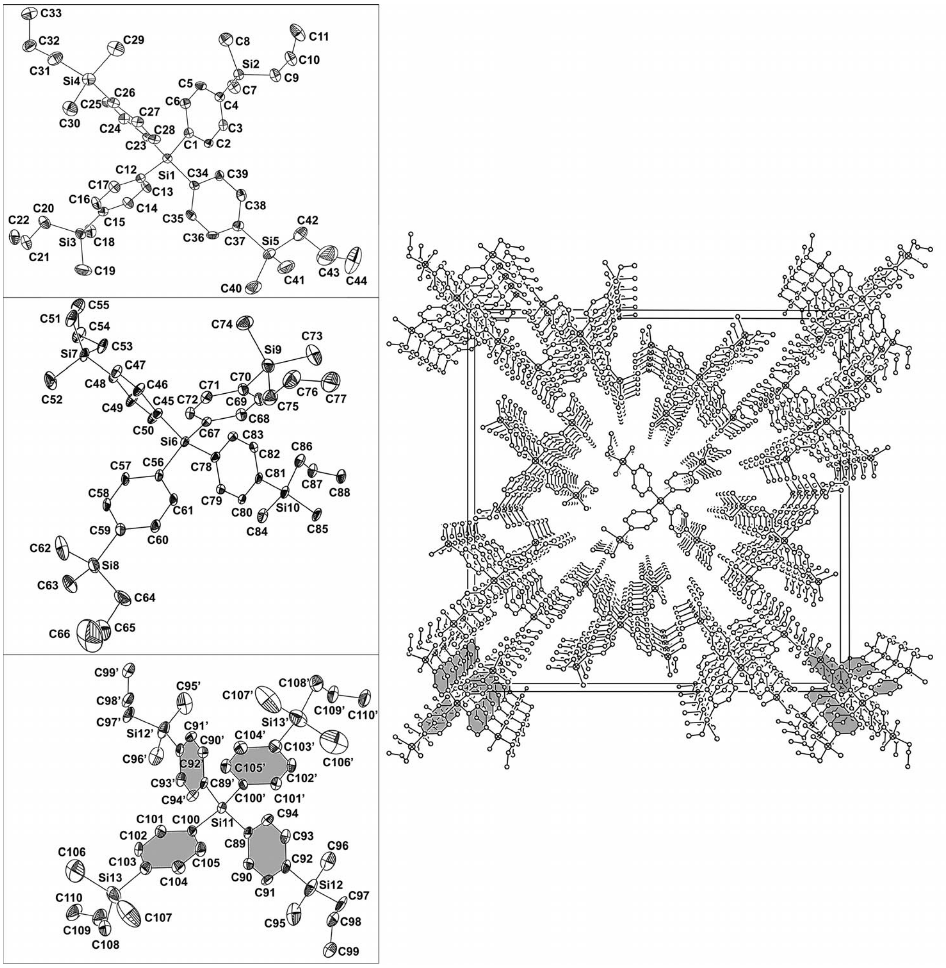

Figure 1. Crystal structure of **7b**: (a) ORTEP diagram (30% probability level) of the molecular structures of the three crystallographically independent molecules of **7b** (left side; top: **7b-I**; middle: **7b-II**; bottom: **7b-III**) and atom-numbering scheme of **7b-I**, **7b-II**, and **7b-III**. (b) Space-filling model of the unit cell showing the arrangement of **7b-I** to **7b-III** in the solid state by formation of three crystallographically independent head-to-head stacking columns along the crystallographic *b* axis. Hydrogen atoms and disordered atoms have been omitted for clarity. Selected bond lengths [Å] and bond angles [°]: Si1–Cl 1.893(6), Si1–C12 1.887(6), Si1–C23 1.888(6), Si1–C34 1.895(6); C1–Si1–C12 112.7(3), C1–Si1–C23 109.1(3), C1–Si1–C34 106.1(3), C12–Si1–C23 108.6(3), C12–Si1–C34 109.1(3), C23–Si1–C34 111.3(3).

are provided in Table S1 (Supporting Information). Selected bond lengths [Å] and bond angles [°] of **7b-I** are summarized in the caption of Figure 1. Related bond lengths and angles of the other crystallographically independent molecules do not differ significantly from these data and are therefore not presented. The bond lengths and bond angles are characteristic of carbosilanes that feature Si–C_6H_4–Si and $SiMe_2(CH_2CH{=}CH_2)$ units, and hence there is no need to discuss these building blocks in more detail.[22]

The 3D network structure of **7b** is set up by nonclassical C–H···π_{CC} hydrogen-bonding (π_{CC} = double bond of the $CH{=}CH_2$ groups; Table S2 in the Supporting Information) and π–π interactions,[23] whereby the centroids of the C=C double bonds can be considered as proton acceptors, of which two types exist: two proton donors–one acceptor (Figure S1, bottom, in the Supporting Information) and one proton donor–one acceptor (Figure S1, top). The 3D network is further stabilized by π–π interactions. Molecules of **7b** form three crystallographically independent head-to-head stacking columns along the crystallographic *b* axis (Figure 1), in which the columns formed by **7b-I** and **7b-II** (Figure 2), are similar with respect to the pattern of the π contacts. Thus, all C_6H_4 building blocks of individual molecules of **7b-I** and **7b-II** are involved in one π–π contact to one phenylene ring of a neighboring molecule. The dis-

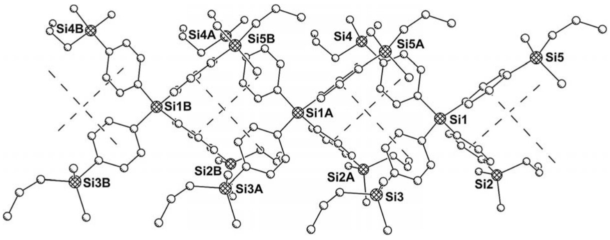

Figure 2. Head-to-head stacking of molecules **7b-I** including π–π interactions between C_6H_4 units of sequenced molecules. Labels A and B refer to atoms that belong to the second and third molecule of **7b-I** along the chain.

tances between the centroids of interacting C_6H_4 units and the interplanar angles (Table S3 in the Supporting Information) fall within the typically observed values for T-shaped benzene stackings.[23a,23b]

One C_6H_4 unit of **7b-III** is involved in two, whereas all other phenylene rings are involved in only one π–π interaction between adjacent molecules (Figure 3). Geometrical details of these contacts (Table S3 in the Supporting Information) are similar to those observed for the chains based on **7b-I** and **7b-II** (Table S3).

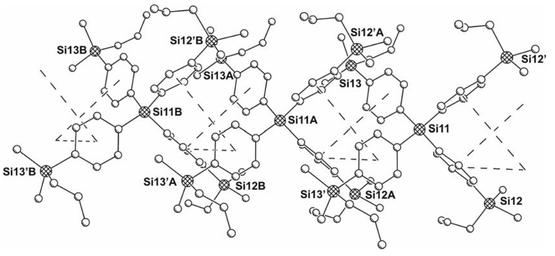

Figure 3. Head-to-head stacking of **7b-III** including π–π contacts between C_6H_4 rings of sequenced molecules. Labels A and B refer to atoms that belong to the second and third molecule of **7b-III** along the chain. Label ′ refers to symmetry-generated atoms, due to crystallographically imposed C_2 symmetry.

Single crystals of **10a** were obtained by vapor-phase diffusion of *n*-pentane into a solution of **10a** in dichloromethane at 25 °C. The structure of **10a** in the solid state is depicted in Figure 4, and the crystal data and structure-refinement parameters are summarized in Table S1 (Supporting Information). For selected bond lengths [Å] and bond angles [°], see Figure 4.

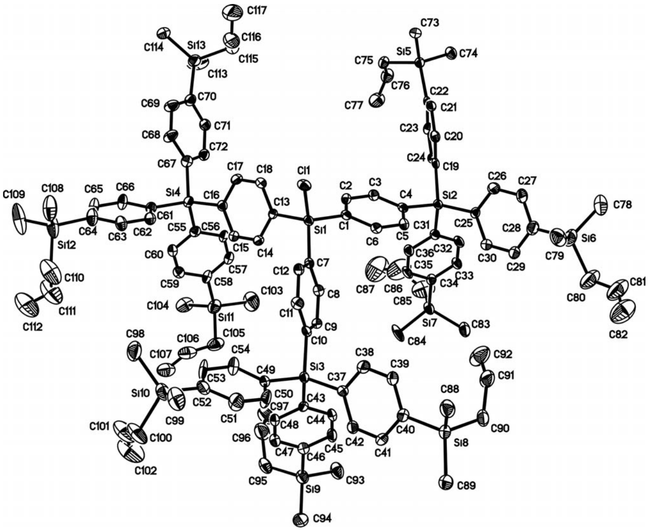

Figure 4. ORTEP diagram (30% probability level) and atom-numbering scheme of **10a**. The hydrogen atoms are omitted for clarity. Selected bond lengths [Å] and bond angles [°]: Si1–Cl1 2.059(3), Si1–C1 1.819(7), Si1–C7 2.005(7), Si1–C13 1.887(7), Si2–C4 1.856(7), Si2–C19 2.014(7), Si2–C25 1.892(8), Si2–C31 1.877(7), Si3–C10 2.003(7), Si3–C37 1.892(8), Si3–C43 1.853(8), Si3–C49 1.854(7), Si4–C16 1.892(8), Si4–C55 1.853(8), Si4–C61 1.854(8), Si4–C67 2.009(8) Si5–C22 2.10(8); C1–Si1–C7 110.6(3), C1–Si1–C13 106.8(3), C7–Si1–C13 116.0(3).

The most striking feature of the molecular structure of **10a** in the solid state is that two molecules of **10a** interdigitate to form self-complementary dimers in the form of a hexagram (Figure 5). Clearly, the geometric parameters of the three crystallographically different arms of **10a** are arranged in a fashion that optimizes interactions of two molecules of **10a**. The dimeric structure is stabilized by π–π interactions through four trimeric phenylene aggregates (Figure 5, top), of which two (**A** and **B**; Figure 5, bottom) are crystallographically independent. In addition, C23–H23···π_{CC} hydrogen bonding participates in stabilizing the dimeric structure (Table S4 in the Supporting Information).[23c–23e] Type-**A** aggregates are set up from a terminal C_6H_4 ring of one molecule of **10a** inserted between two terminal C_6H_4 units from another molecule of **10a**, whereas type-**B** aggregates are formed by one inner phenylene moiety of **10a** inserted between two terminal C_6H_4 rings of another molecule (Figure 5). Both aggregates correspond to T-shaped benzene dimers (Figure 5).[23a,23b] The tendency of **10a** to form self-complementary dimers through π–π interactions is also verified by the Si–C_{Ar} distances. According to the CCD database, only two examples are known with Si–C_{Ar} distances longer than 2.0 Å.[24] In **10a**, the Si4–C67 [2.009(8) Å] and Si2–C19 [2.014(7) Å] distances are elongated relative to the other Si2–C_{Ar} and Si4–C_{Ar} bonds (Figure 4). In **B**, the Si–C_{Ar} bonds of the intercalating C_6H_4 rings are exceptionally lengthened relative to those of type-**A** assemblies, which most clearly is attributed to the optimization of π–π interactions between two molecules of **10a**. The hexagrams form stacks on the basis of further cross-linkage by means of C–H···π_{CC} arrangements (one proton donor–one proton acceptor) to form the three-dimensional structure (Table S4).

The electrostatic potentials of **7b** and **10a** (Figure 6) were calculated by using the DFT/B3LYP theory with a 6-31g(d) basis set on all atoms [(d) = d functions added to heavy atoms].[25,26] In **7b**, the most negative electrostatic potential values are around the C=C double bonds, whereas the most positive values are found around the hydrogen atoms (Figure 6A). The observed C–H···π_{CC} contacts and the second-most-negative electrostatic potential values around the aromatic π systems rationalize the π–π interactions. A similar behavior is observed for **10a** (Figure 6B and C). Also, the electrostatic potential values around Cl indicate the presence of less negative potentials end-capped along the Si1–Cl1 bond (green color, Figure 6C), whereas the potential values are more negative in the π region of the atom. The anisotropy of the electrostatic potential around covalently bonded chlorine atoms is known in the literature.[25a,25b] On the basis of electrostatic laws, these potential surfaces render the formation of the reported weak intermolecular interactions inanimate.

The IR spectra of the allyl-end-grafted carbosilanes **7**, **8** and **10**–**12** show characteristic absorptions at approximately 1630 cm^{-1} for the $\nu_{C=C}$ vibrations. In the range of 800–840 cm^{-1}, bands for the Si–C units are found, which is in agreement with allyl-functionalized carbosilanes. The Si–CH_3 moieties absorb at 1250 cm^{-1} (Si–CH_3 bending).[27]

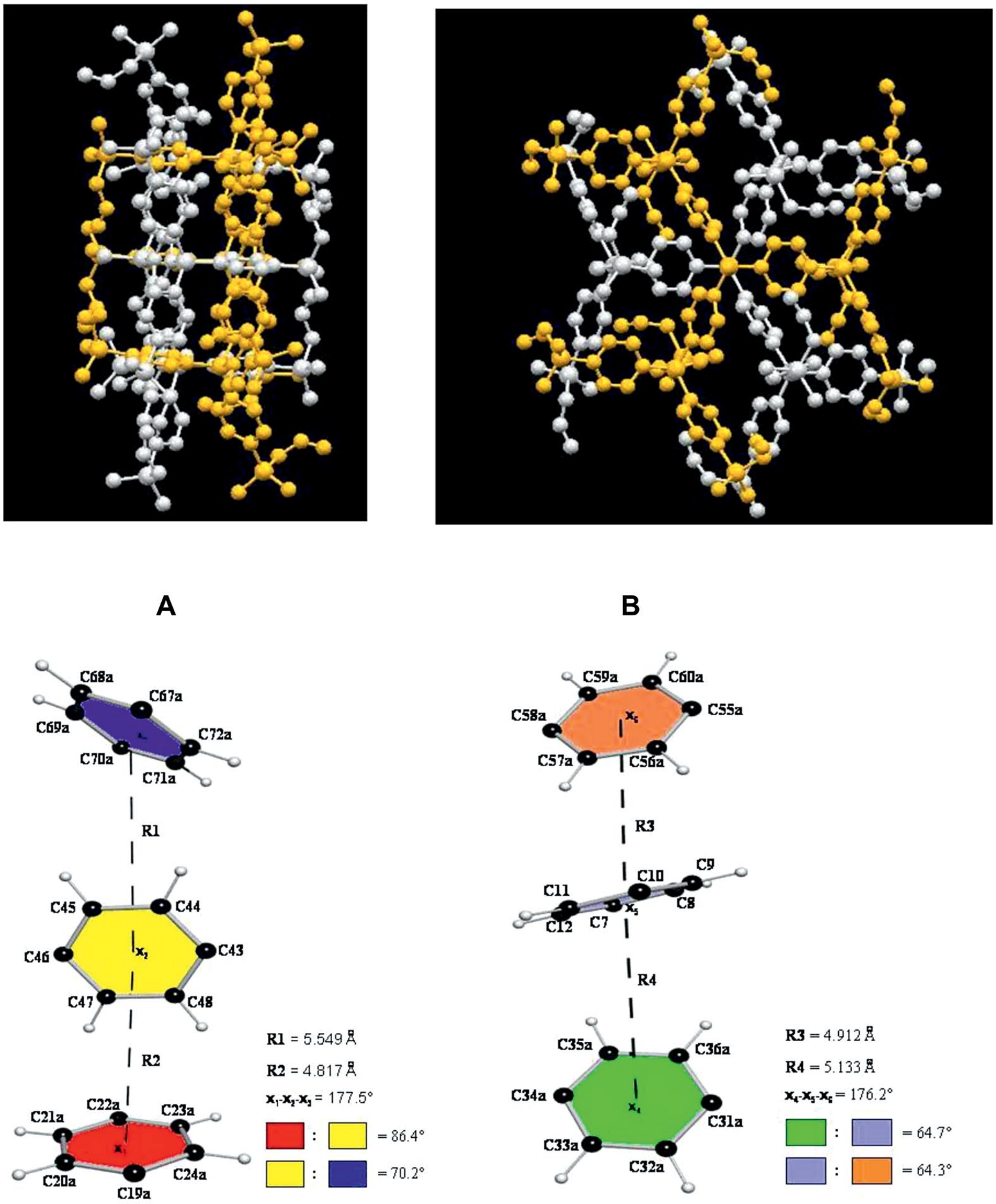

Figure 5. Top: side view of the dimeric structure of **10a** (left). The dimer viewed along the axis that connects the chlorine and its symmetry-equivalent atom (right). The two molecules are colored by symmetry operation (inversion center). Bottom: structural details of the two crystallographically different aggregates **A** and **B** formed by π–π interactions of dimeric **10a**.

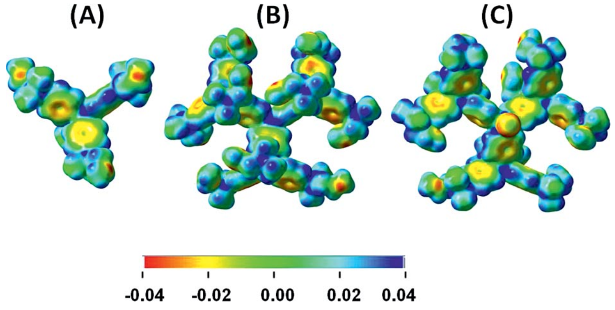

Figure 6. Calculated electrostatic potential surfaces of (A) **7b** and (B, C) **10a** [in (B), the chlorine atom is directed away from the viewer; in (C), the chlorine atom is directed towards the viewer]. The electron density contour isovalue is set to 0.005. Units of the colored scale are in atomic units.

For NMR spectroscopic assignment, the atom-numbering scheme of the respective molecules is depicted in Figure S3 (Supporting Information). The ^{1}H NMR spectra of **7a**–**7d** and **8a**–**8d** show well-resolved resonance signals, as is expected for the respective organic groups (see the Experimental Section). In contrast, the ^{1}H NMR spectra of the first-generation dendrimers **10**–**12** show additional signals for each organic group with a strong dependence on concentration, solvent, and temperature [i.e., the $SiCH_3$ moieties of **12b** in $CDCl_3$ show that the ratio of the relative integrals of the high- to low-field signals decreases with decreasing concentration (Figure 7b) and increasing temperature (Figure 7c)]. This indicates that **12b** forms a mixture of monomeric and self-associated dimeric species in solution. As depicted in Figure 7b and c, the high-field signal is related to self-associated species, whereas the downfield signal can be assigned to the monomeric form. The high-field shift of the resonance signals can be explained by the presence of the respective signals in a more shielded anisotropic environment inside the self-associated species relative to the chloroform environment for the monomer. Other organic groups in **12b** show a behavior similar to the $SiCH_3$ groups, however, it is impossible to completely analyze them due to spectral multiplicity (see the Experimental Section).

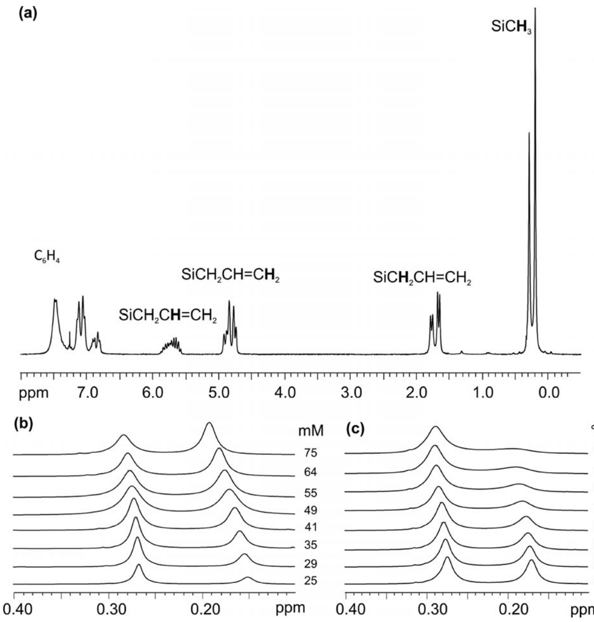

Figure 7. (a) ^1H NMR spectrum of **12b** in $CDCl_3$ with a concentration of 75 mM at 25 °C. (b) Concentration dependence of the $SiCH_3$ region (25–75 mM) at 25 °C. (c) Temperature dependence of the $SiCH_3$ region in the range of 25–53 °C at 49 mM.

The ^1H NMR spectroscopic measurements of **12b** were repeated in [D$_6$]benzene, because it is supposed that an aromatic solvent will reduce the concentration of the self-associated species through competition of π–π interactions (Figure 8).[28] It was found that the high-field signal for the self-associated system ($SiCH_3$) in $CDCl_3$ (Figure 8c, signal labeled with D) is reduced to a low-field shoulder in [D$_6$]benzene (Figure 8a and b), which supports π–π interactions for the self-associated species. As expected, upon decreasing the concentration and increasing the temperature to 75 °C, the shoulder disappeared (Figure 8b, label D, Figure 8d). The appearance of the self-associated system as a low-field shoulder relative to the signal of the monomeric form is attributed to a weaker aromatic shielding environment inside the self-associated system than the aromatic shielding environment of the benzene solvent around the monomer.

To determine the structure of the self-associated species, molecular mechanics calculations were performed with the MM$^+$ force field as implemented in HyperChem 4.0^2. The optimized structure of carbosilane **12b** is shown in Figure 9a and the dimer as self-complementary structure in Figure 9b. The optimized dimeric structures for **10a**, **10b**, **11a**, **11b**, and **12b**–**12d** display the same π–π interactions (type **A** and **B** phenylene aggregates) as already observed for **10a** in the solid state (Figure 5). The estimated core-silicon–core-silicon distance for the **12b** dimer is 6.957 Å, whereas for dimeric **10a** it is 7.094 Å. The molecular mechanical optimization data fit very well with the obtained solid-state self-complementary structure of **10a** (core-silicon–core-silicon distance 6.572 Å; Figure 5).

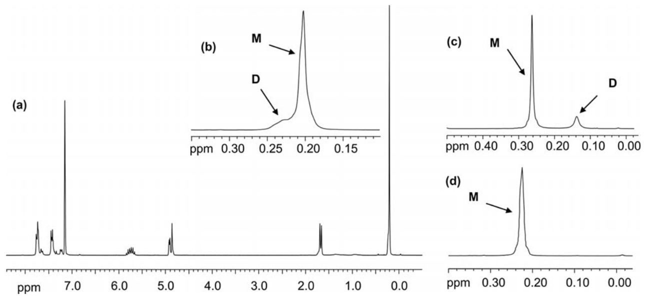

Figure 8. (a) ^1H NMR spectrum of **12b** in C_6D_6 with a concentration of 12 mM at 25 °C. (b) ^1H NMR region for the methyl groups from spectrum (a). (c) ^1H NMR spectroscopic signals for the methyl groups of **12b** in $CDCl_3$ (12 mM, 25 °C). (d) ^1H NMR spectroscopic region for the methyl groups in C_6D_6 at 75 °C. Label M refers to the monomer and D to the dimer.

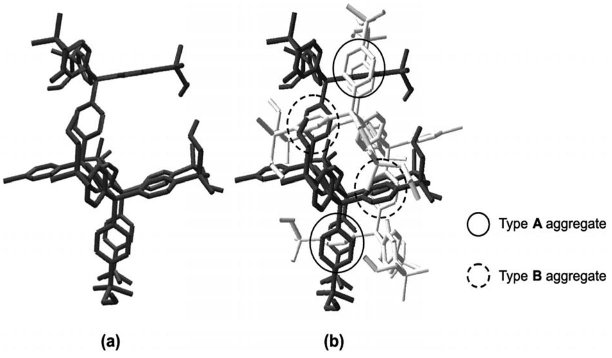

Figure 9. Optimized structure of (a) monomeric carbosilane **12b** and (b) its self-complementary structure.

The proof for the self-complementary structure of **12b** in solution, suggested by MM$^+$ calculations, is obtained from ^1H NMR spectroscopic studies. Figure 10 shows the ^1H NMR spectra of **12b** at 75 °C in C_6D_6 and at –80 °C in CD_2Cl_2. It is expected that the monomeric species predominates at high temperature in benzene; it shows three different signals for the phenylene groups (BrC_6H_4Si, inner and outer SiC_6H_4Si) and only one type of methyl and allyl groups (see the Experimental Section). In the self-complementary structure (Figure 9b), rotational restrictions result in the splitting of the nine outer SiC_6H_4Si units: three of them are directed towards the other complementary molecule, whereas six SiC_6H_4Si groups are oriented away from it. The ^1H NMR spectroscopic signals of these groups at –80 °C have a ratio of 4:24:12:12 (Figure 10b), which fits with the self-complementary, dimeric structure (Figure 9b).

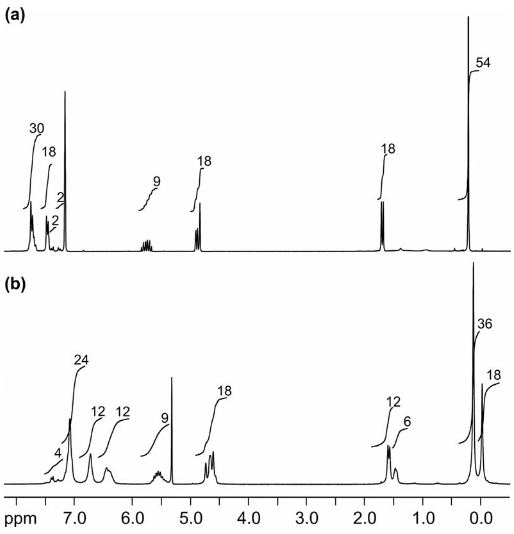

Figure 10. ^{1}H NMR spectra of **12b**: (a) measured in C_6D_6 (12 mM) at 75 °C and (b) in CD_2Cl_2 (12 mM) at –80 °C.

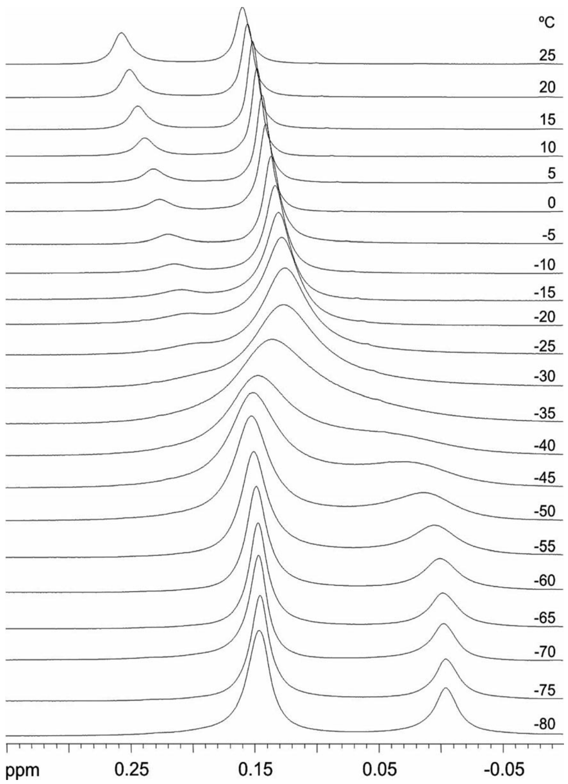

Figure 11. Temperature dependence of the $SiCH_3$ proton signals of **12b** in the temperature range of –80 to 25 °C (CD_2Cl_2, c = 12 mM).

Similar to the outer SiC_6H_4Si units, the nine terminal $-Si(CH_3)_2(CH_2CH=CH_2)$ groups are split into two sets (Figure 9b). This analysis fits with the ^{1}H NMR spectrum measured at –80 °C, which shows two types for the $SiCH_3$ protons (ratio 36:18) and two arrays for the allyl $SiCH_2$ protons (ratio 12:6). The signals of the three terminal $-Si(CH_3)_2(CH_2CH=CH_2)$ units inside the dimer are observed at higher field than those of the six terminal $Si(CH_3)_2(CH_2CH=CH_2)$ moieties (see the Experimental Section). This can be explained by a shielding of the C_6H_4 rings inside the dimer relative to the CD_2Cl_2 environment at the surface (Figures 9b and 10b).

In the ^{1}H NMR spectrum of **12b**, only the dimeric species exists in CD_2Cl_2 at –80 °C. To understand the monomer formation from the appropriate dimer, a series of ^{1}H NMR spectra were measured between –80 and 25 °C in steps of 5 °C. For simplicity, only the signals of the $SiCH_3$ protons are shown in Figure 11. At –80 °C, two well-separated signals in a ratio of 2:1 as expected for the dimer are observed (Figure 9a). Coalescence is observed at –30 °C (Figure 11). Close to this temperature, a new signal at lower field for the monomer appeared. The integration ratio of the CH_3 signals (monomer versus dimer) increases with rising temperature (Figure 11), which can be explained by the number of the dimeric species that have sufficient kinetic energy to separate into the monomers with freely rotating $-C_6H_4$-4-$Si(CH_3)_2(CH_2CH=CH_2)$ units at higher temperature. As the monomer concentration increases, the relative integration of this signal relative to the dimer increases continuously (Figure 11, –30 to +25 °C).

The ^{1}H NMR spectrum of **12b** in nonaromatic solvents (e.g., $CDCl_3$) features two signal categories, one of which corresponds to the monomer and the other to the dimer (Figure 9). Figure 12 shows the analysis of the signal behavior for the methyl groups in terms of its dependence on temperature and concentration for **11a**, **11b**, **12b**, and **12c**. As can be seen, the intensity of the methyl signals (upward-facing arrow) between δ = 0.25 and 0.27 ppm increases with rising temperature and decreasing concentration as allocated to the monomer. On the other hand, the methyl signals with a downward-facing arrow have a relative integration that decreases with increasing temperature and decreasing concentration and can be assigned to the dimer.

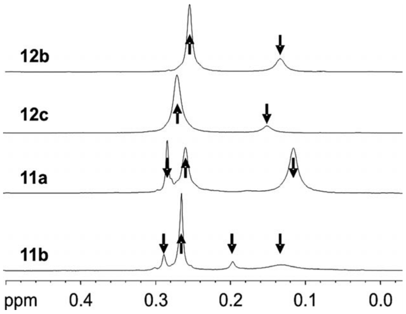

Figure 12. Comparison of the behavior of the methyl signals for **11a**, **11b**, **12b**, and **12c** [up arrow (↑): integration increases (monomer formation); down arrow (↓): integration decreases (dimer) with increasing temperature and decreasing concentration].

A detailed analysis of the dimerization process for **11a**, **11b**, **12b**, and **12c** was achieved by thermodynamic studies (Supporting Information). As expected, these processes are enthalpy-favored and entropy-opposed. According to the structure analysis of **10a** in the solid state, the favorable enthalpy is provided by π–π interactions between 1,4-phenylene units. This is also supported by the effect of the aromatic solvent (i.e., [D$_6$]benzene). Aromatic solvents reduce the appropriate π–π interactions,[28] which consequently reduces the dimer formation (e.g., **12b**; Figures 8 and 10a). The free-energy Δ*G* values for the dimerization of **11a**, **11b**, **12b**, and **12c** are, at –0.9 to –3.7 kcal mol^{-1}, small. In terms of experimental error, the binding enthalpies of all four compounds are similar. However, the obtained values indicate that the binding enthalpy is slightly smaller for **11a** and **11b** than **12b** and **12c** (Table S5 in the Supporting Information). This can be explained by the presence of $Si[C_6H_4–4-Si(CH_3)_{3-n}(CH_2CH=CH_2)_n]_3$ groups in **11a** and **11b**, which produce larger steric repulsion with intercalated arms from the second molecule (Figure 9b) than the bromo substituent present in **12b** and **12c**, respectively. Nevertheless, the smaller entropic loss for **11a** and **11b** with respect to **12b** and **12c** is responsible for the large increase in the dimerization constant of **11a** and **11b** (Table S5). The highly ordered monomers of **11a** and **11b** relative to the monomers of **12b** and **12c** are responsible for the small entropy loss for the dimerization of **11a** and **11b**.

Distinctive resonance signals are also observed for all organic groups in the $^{13}C\{^1H\}$ NMR spectra (see the Experimental Section). The $^{13}C\{^1H\}$ NMR spectra of the first-generation carbosilanes **10**–**12** show characteristic features through some signal splitting and broadening (see above). Due to dimerization processes, the analysis was achieved by ^{13}C-DEPT-135 experiments and a comparison with the spectral interpretation of the zeroth-generation compounds **7** and **8** (see the Experimental Section). However, it was not possible to assign all of the carbon signals due to complication of broadening and splitting that resulted from dimerization processes. For **11b** and **12c**, the signal splitting is, however, only observed for the $SiCH_3$ and $=CH_2$ units (see the Experimental Section). The $^{13}C\{^1H\}$ NMR spectroscopic signals for the $SiCH_3$ and $SiCH_2CH=CH_2$ groups of the first-generation carbosilanes show similar chemical shifts to those observed for the zeroth-generation compounds.

All carbosilanes show for the hydrogen-bearing carbon atoms of the terminal SiC_6H_4Si units resonances at δ = 133.2 and 135.5 ppm, respectively. In **11a**, **11b**, and **12c**, they are split into two signals that are explained by the monomeric and dimeric form present in solution (see above). Moreover, the chemical shifts of the outer CSi carbon atoms of the terminal SiC_6H_4Si units are directly affected by the substituent attached to Si. For example, the respective carbon atom resonates at δ = 142.2 ppm in carbosilanes that have three methyl groups attached to the silicon atom, for example, **8a**. This signal undergoes a high-field shift, when the methyl groups are subsequently replaced by allyl units (i.e., **8d**; see the Experimental Section). For **11a** and **12b**, this resonance is split into two signals due to dimerization processes. On the contrary, the inner CSi carbon atoms of the terminal SiC_6H_4Si units have a similar chemical shift at $\delta \approx$ 134.4 ppm (see the Experimental Section).

In the $^{29}Si\{^1H\}$ NMR spectra of the zeroth-generation compounds, a resonance signal is found at $\delta \approx$ –14.5 ppm for the inner silicon atom, which is in accordance with tetraphenylsilanes.[29] The Si atoms of the terminal $SiMe_{3-n}(CH_2CH=CH_2)_n$ units are observed at δ = –3.7 (*n* = 0), –4.2 (*n* = 1), –5.6 (*n* = 2), and –7.8 ppm (*n* = 3), respectively. The $^{29}Si\{^1H\}$ NMR spectra of **10a** and **10b** in $CDCl_3$ at 298 K show three characteristic Si signals: $Si(C_6H_4)_4$ at $\delta \approx$ –14.7 ppm,[29] $SiMe_{3-n}(CH_2CH=CH_2)_n$ at δ = –4.6 (**10a**) or –5.8 ppm (**10b**) and $SiCl(C_6H_4)_3$ at δ = –12.8 ppm. The $^{29}Si\{^1H\}$ NMR spectra of **12c** and **12d** were measured in $CDCl_3$ at 55 and 50 °C, respectively, whereas the $^{29}Si\{^1H\}$ NMR spectra of **12b** (20 °C), **11a** (75 °C), and **11b** (75 °C) were determined in C_6D_6. For the core and inner silicon atoms two signals (**12b**, **12c**, and **12d**) or one broad resonance (**11a**, **11b**) are found in the range of δ = –14.8 to –13.3 ppm, whereas the terminal $SiMe_{3-n}(CH_2CH=CH_2)_n$ units show resonances at $\delta \approx$ –5.0 ppm for **12b** and **11a**, at $\delta \approx$ –6.0 ppm for **12c** and **11b**, and at δ = –8.0 ppm for **12d**.

ESI-TOF mass spectrometric measurements for **7** and **8** showed the respective molecular ion peaks $[M + K]^+$, when doped with K^+. Carbosilanes **10a**, **11a**, and **12b** were studied by MALDI-TOF mass spectrometry. For dendrimers **11a** and **12b**, the molecular ion peaks $[M + Ag]^+$ in a nitroanthracene matrix (promoted by [AgOTf]) were observed. For **10a** with an [AgOTf] promoter in a 2,5-dihydroxybenzoic acid matrix, an ion peak at *m*/*z* = 2069.7 was found that can be assigned to $[M + (HO)_2C_6H_4CO_2H – Cl]^+$.

Conclusion

In this work, 1,4-phenylene was used as a building block in the convergent synthesis of a new class of zeroth- and first-generation carbosilane dendrimers with dense shell structures. The rigidity of the phenylene group provides these molecules with some advantages over well-known carbosilane dendrimers with flexible aliphatic units (i.e., in homogeneous catalysis). The crystal structures of two dendritic carbosilanes (**7b**, **10a**) illustrate that self-assembly of these molecules is controlled by $C–H\cdots\pi_{CC}$ (π_{CC} = C=C double bond of the $CH=CH_2$ groups) and π–π interactions between C_6H_4 units that interact with each other exclusively in a T-shaped fashion.

The zeroth-generation dendrimer **7b** shows 1D head-to-head stacked columns that are aggregated further to form a 3D network structure. On the other hand, the π–π interactions observed for **10a** in the solid state induce the formation of a unique self-complementary six-pointed star dimer, which is stabilized by four trimeric C_6H_4 aggregates to result in a total of eight π–π interactions. The calculated electrostatic potential surfaces rationalize the formation of $C–H\cdots\pi_{CC}$ as well as π–π interactions. Also, the calculated electrostatic potential indicated that the double bond is a better proton acceptor than the aromatic π system, which agrees with the observed solid-state self-assembly of **7b** and **10a**. Additionally, molecular mechanics calculations (MM^+), which were performed for the first-generation carbosilanes **10**–**12**, propose similar self-complementary dimeric structures. The formation of dimers was proven by dynamic NMR spectroscopic studies. Geometries closer to the globular shape enhance the dimerization, whereas the replacement of methyl by larger allyl units inhibits it due to steric effects.

Experimental Section

General: All reactions were carried out under nitrogen by using standard Schlenk techniques. Solvents and reagents were purified and dried by distillation. Diethyl ether, *n*-hexane, *n*-pentane, and tetrahydrofuran were heated to reflux with sodium/benzophenone ketyl, distilled, and saturated with nitrogen. The chlorosilanes were distilled from magnesium prior to use, and TMEDA was heated to reflux with calcium hydride, distilled, and saturated with nitrogen. All other chemicals were purchased from commercial suppliers and were used as received. IR spectra were recorded with a Perkin–Elmer FTIR 1000 spectrometer as films between NaCl plates or as KBr discs. ^{1}H, ^{13}C{^{1}H}, and ^{29}Si{^{1}H} NMR spectra were recorded with a Bruker Avance 250 spectrometer operating in the Fourier transform mode. ^{1}H NMR spectra were recorded at 250.130 MHz [internal standard relative to $CDCl_3$ (δ = 7.26 ppm) and C_6D_6, (7.16 ppm)]; ^{13}C{^{1}H} NMR spectra were recorded at 62.902 MHz [internal standard relative to $CDCl_3$ (δ = 77.0 ppm) and C_6D_6 (128.4 ppm)]; ^{29}Si{^{1}H} NMR spectra were recorded at 49.692 MHz [external standard relative to $SiMe_4$ (δ = 0.0 ppm)]. The assignment of ^{13}C{^{1}H} and ^{29}Si{^{1}H} NMR spectroscopic signals is mainly based on ^{13}C-DEPT-135 spectra and 2D-correlation spectra [gradient with sensitivity-enhanced heteronuclear multiple quantum correlation (gs-HMQC) for carbon and silicon and gradient with sensitivity-enhanced heteronuclear multiple bond correlation (gs-HMBC) for carbon]. ESI-TOF mass spectra were recorded with a Mariner Biospectrometry Workstation 4.0 (Applied Biosystems) with dichloromethane as solvent and potassium thiocyanate for doping. MALDI-TOF mass spectra were performed with a Voyager-DE PRO Biospectrometry Workstation (Applied Biosystems) with nitroanthracene as matrix (**11a** and **12b**) or 2,5-dihydroxybenzoic acid (**10a**) and silver triflate as promoter. C and H microanalyses were performed with a Foss Heraeus Vario EL analyzer. Melting points of pure samples were measured with a Gallenkamp MFB 595 010 equipment. Molecular mechanics calculations were performed with the MM^{+} force field as implemented in HyperChem 4.0^{2}. DFT/B3LYP calculations: the atomic coordinates of **7b** and **10a** were taken from the crystal structure. Gaussian 03 was used for electronic energy calculations.[26]

Synthesis of 1-Br–C_6H_4–4-$SiMe_{3-n}(CH_2CH{=}CH_2)_n$ (5a,[17] *n* = 1; 5b, *n* = 2; 5c,[18] *n* = 3)

General Method: Allylmagnesium bromide was prepared by slow addition of allyl bromide ($n \times 1.00$ mol, $n \times 120.98$ g) dissolved in diethyl ether ($n \times 1000$ mL) to a suspension of magnesium turnings ($n \times 1.50$ mol, $n \times 36.45$ g) in diethyl ether (120 mL) for 8 h. After 2 h of stirring, the allylmagnesium bromide was transferred with a cannula from the excess amount of magnesium. 1-Br–C_6H_4–4-$SiMe_{3-n}Cl_n$ dissolved in diethyl ether (200 mL) was added dropwise to this solution over 2 h. The obtained reaction mixture was heated to reflux for 5 h and then quenched with a 10% aqueous HCl solution (250 mL). The organic layer was extracted with water (200 mL), dried with magnesium sulfate, and concentrated in an oil-pump vacuum to give crude 1-Br–4-[$SiMe_{3-n}(CH_2CH{=}CH_2)_n$]-$C_6H_4$. See the literature for spectroscopic and analytical data for **5a**[17] and **5c**.[18]

Data for 5b: Purified by fractional vacuum distillation. Yield (93.50 g, 0.33 mol, 33%) of a colorless liquid. B.p. 96 °C/0.5 Torr. ^{1}H NMR ($CDCl_3$): δ = 7.50 (dt, *J* = 8.20, 1.84 Hz, 2 H, H^{2}), 7.37 (dt, *J* = 8.20, 1.84 Hz, 2 H, H^{3}), 5.75 (m, 2 H, H^{6}), 4.89 (m, 2 H, H^{7}), 4.87 (m, 2 H, H^{7}), 1.80 (dt, *J* = 8.08, 1.15 Hz, 4 H, H^{5}), 0.29 (s, 3 H, H^{8}) ppm. ^{13}C{^{1}H} NMR ($CDCl_3$): δ = 135.6 (1 C^{4}), 135.5 (2 C^{3}), 133.7 (2 C^{6}), 130.9 (2 C^{2}), 124.1 (1 C^{1}), 114.2 (2 C^{7}), 21.4 (2 C^{5}), –5.9 (1 C^{8}) ppm. ^{29}Si{^{1}H} NMR ($CDCl_3$): δ = –5.3 (1 Si^{1}) ppm. IR (NaCl): $\tilde{\nu}$ = 3076, 3050, 2993, 2971, 2905, 2885, 1630 (m, C=C), 1254 (m, CH_3 bending), 820 (s, Si–C), 803 (s, Si–C) cm^{-1}. $C_{13}H_{17}BrSi$ (281.26): calcd. C 55.51, H 6.09; found C 55.45, H 6.08.

Tetrakis{4-[diallyl(methyl)silyl]phenyl}silane (7c): *n*BuLi (2.5 M, 11.85 mmol, 4.74 mL, *n*-hexane) was added dropwise to **5b** (11.85 mmol, 3.33 g) dissolved in diethyl ether (60 mL) at –30 °C. The reaction mixture was stirred below –10 °C for 30 min, and then $SiCl_4$ (8.50 mmol, 1.444 g, 0.98 mL) was added in a single portion. The reaction mixture was stirred at this temperature for 30 min and then at 25 °C for 24 h. Afterwards, it was quenched with water (100 mL), and the resulting mixture was extracted with diethyl ether (100 mL). The organic layer was dried with magnesium sulfate, and all volatile materials were removed in an oil-pump vacuum. The crude product was purified by silica gel column chromatography (*n*-hexane/20% dichloromethane/*n*-hexane; column size: 4 × 25 cm) to give **7c** (0.850 g, 1.020 mmol, 34%) as a colorless solid. M.p. 237 °C. ^{1}H NMR ($CDCl_3$): δ = 7.53 [m, 8 H (H^{2}) + 8 H (H^{3})], 5.79 (ddt, *J* = 16.86, 10.18, 8.06 Hz, 8 H, H^{6}), 4.90 (ddt, *J* = 16.86, 2.76, 1.50 Hz, 8 H, H^{7}), 4.87 (ddt, *J* = 10.10, 2.76, 1.50 Hz, 8 H, H^{7}), 1.82 (dt, *J* = 8.06, 1.50 Hz, 16 H, H^{5}), 0.29 (s, 12 H, H^{8}) ppm. ^{13}C{^{1}H} NMR ($CDCl_3$): δ = 138.6 (4 C^{4}), 135.5 (8 C^{2}), 134.9 (4 C^{1}), 134.1 (8 C^{6}), 133.2 (8 C^{3}), 113.9 (8 C^{7}), 21.5 (8 C^{5}), –5.9 (4 C^{8}) ppm. ^{29}Si{^{1}H} NMR ($CDCl_3$): δ = –14.8 (1 Si^{1}), –5.8 (4 Si^{2}) ppm. IR (KBr): $\tilde{\nu}$ = 3070, 3047, 2989, 2967, 2907, 2878, 1630 (s, C=C), 1252 (m, CH_3 bending), 1132, 820 (s, Si–C), 805 (s, Si–C) cm^{-1}. ESI-TOF: *m*/*z* (%) = 871.39 (10) [M + K]$^{+}$. $C_{52}H_{68}Si_5$ (833.52): calcd. C 74.93, H 8.22; found C 74.85, H 8.24.

1-Bromo-4-{tris[4-(trimethylsilyl)phenyl]silyl}benzene (8a): *n*BuLi (2.5 M, 25.2 mmol, 10.08 mL, *n*-hexane) was added dropwise to **3a** (25.2 mmol, 2.310 g) dissolved in diethyl ether (100 mL) at –30 °C. The reaction mixture was stirred below –10 °C for 30 min, then TMEDA (37.8 mmol, 4.393 g, 5.71 mL) was added, and stirring was continued for 5 min. A solution of **3d** (8.0 mmol, 2.324 g) in diethyl ether (40 mL) was added, and the reaction mixture was stirred at –10 °C for 30 min and at 25 °C for 24 h. The reaction solution was quenched with water (50 mL), and the resulting mixture was extracted with diethyl ether (100 mL). The organic layer was dried with magnesium sulfate, and all volatiles were removed in an oil-pump vacuum. The crude product was purified by silica gel column chromatography (*n*-hexane; column size: 4 × 35 cm) to afford **8a** (3.286 g, 5.20 mmol, 65%) as a colorless solid. M.p. 221 °C. ^{1}H NMR ($CDCl_3$): δ = 7.53 [s, 6 H (H^{6}) + 6 H (H^{7})], 7.52 (dt, *J* = 8.5, 1.75 Hz, 2 H, H^{2}), 7.44 (dt, *J* = 8.5, 1.75 Hz, 2 H, H^{3}), 0.28 (s, 27 H, H^{9}) ppm. ^{13}C{^{1}H} NMR ($CDCl_3$): δ = 142.2 (3 C^{8}), 138.0 (2 C^{3}), 135.5 (6 C^{3}), 133.9 (3 C^{5}), 133.3 (1 C^{4}), 132.7 (6 C^{7}), 131.0 (2 C^{2}), 124.6 (1 C^{1}), –1.2 (9 C^{9}) ppm. ^{29}Si{^{1}H} NMR ($CDCl_3$): δ = –14.6 (1 Si^{1}), –3.9 (3 Si^{2}) ppm. IR (KBr): $\tilde{\nu}$ = 3050, 2996, 2954, 2892, 1249 (s, CH_3 bending), 1133, 839 (s, Si–C) cm^{-1}. ESI-TOF: *m*/*z* (%) = 669.13 (80) [M + K]$^{+}$. $C_{33}H_{43}BrSi_4$ (631.94): calcd. C 62.72, H 6.86; found C 62.48, H 7.09.

1-Bromo-4-{tris[4-(allyldimethylsilyl)phenyl]silyl}benzene (8b): The same procedure as in the preparation of **8a** was used for the synthesis of **8b**: *n*BuLi (2.5 M, 27.02 mmol, 10.80 mL, *n*-hexane), **5a** (27.02 mmol, 6.890 g) in diethyl ether (100 mL), TMEDA (40.53 mmol, 4.710 g, 6.101 mL), and **3d** (8.58 mmol, 2.492 g) in diethyl ether (40 mL). The crude product was purified by silica gel column chromatography (*n*-hexane; column size: 4 × 35 cm) to afford **8b** (3.580 g, 5.04 mmol, 59%) as a colorless solid. M.p. 102 °C.

^{1}H NMR (CDCl$_3$): δ = 7.53 [s, 6 H (H^{6}) + 6 H (H^{7})], 7.53 (dt, *J* = 8.33, 1.74 Hz, 2 H, H^{2}), 7.43 (dt, *J* = 8.33, 1.74 Hz, 2 H, H^{3}), 5.79 (ddt, *J* = 16.65, 10.37, 8.06 Hz, 3 H, H^{10}), 4.88 (ddt, *J* = 16.65, 2.69, 1.06 Hz, 3 H, H^{11}), 4.86 (ddt, *J* = 10.37, 2.69, 1.06 Hz, 3 H, H^{11}), 1.77 (dt, *J* = 8.05, 1.06 Hz, 6 H, H^{9}) 0.29 (s, 18 H, H^{12}) ppm. ^{13}C{^{1}H} NMR (CDCl$_3$): δ = 140.5 (3 C^{8}), 137.9 (2 C^{3}), 135.5 (6 C^{6}), 134.5 (3 C^{10}), 134.2 (3 C^{5}), 133.1 (1 C^{4}), 133.0 (6 C^{7}), 131.1 (2 C^{2}), 124.7 (1 C^{1}), 113.5 (3 C^{11}), 23.5 (3 C^{9}), –3.6 (6 C^{12}) ppm. ^{29}Si{^{1}H} NMR (CDCl$_3$): δ = –14.6 (1 Si^{1}), –4.6 (3 Si^{2}) ppm. IR (KBr): ṽ = 3070, 3048, 2989, 2953, 2908, 2885, 1629 (m, C=C), 1249 (m, CH$_3$ bending), 1133, 836 (s, Si–C), 802 (s, Si–C) cm^{-1}. ESI-TOF: *m*/*z* (%) = 749.19 (100) [M + K]$^{+}$. $C_{39}H_{49}BrSi_4$ (710.05): calcd. C 65.97, H 6.96; found C 65.81, H 6.72.

1-Bromo-4-{tris[4-(diallylmethylsilyl)phenyl]silyl}benzene (8c): The same procedure as in the preparation of **8a** was used to prepare **8c**: *n*BuLi (2.5 M, 40.5 mmol, 16.5 mL, *n*-hexane), **5b** (40.46 mmol, 11.37 g) in diethyl ether (150 mL), TMEDA (60.75 mmol, 7.047 g, 9.13 mL), and **3d** (12.85 mmol, 3.731 g) in diethyl ether (60 mL). Silica gel column chromatography (*n*-hexane/20% dichloromethane/*n*-hexane; column size: 4 × 45 cm) afforded **8c** (7.150 g, 9.072 mmol, 71%) as a colorless solid. M.p. 99 °C. ^{1}H NMR (CDCl$_3$): δ = 7.55 [s, 6 H (H^{6}) + 6 H (H^{7})], 7.54 (dt, *J* = 8.18, 1.72 Hz, 2 H, H^{2}), 7.44 (dt, *J* = 8.18, 1.72 Hz, 2 H, H^{3}), 5.81 (ddt, *J* = 16.86, 10.17, 8.05 Hz, 6 H, H^{10}), 4.92 (ddt, *J* = 16.86, 2.22, 1.31 Hz, 6 H, H^{11}), 4.90 (ddt, *J* = 10.17, 2.22, 1.31 Hz, 6 H, H^{11}), 1.76 (dt, *J* = 8.05, 1.31 Hz, 12 H, H^{9}), 0.32 (s, 9 H, H^{12}) ppm. ^{13}C{^{1}H} NMR (CDCl$_3$): δ = 138.9 (3 C^{8}), 137.9 (2 C^{3}), 135.4 (6 C^{6}), 134.3 (3 C^{5}), 134.0 (6 C^{10}), 133.3 (6 H^{7}), 133.0 (1 C^{4}), 131.0 (2 C^{2}), 124.8 (1 C^{1}), 114.0 (6 C^{11}), 21.5 (6 C^{9}), –5.9 (3 C^{12}) ppm. ^{29}Si{^{1}H} NMR (CDCl$_3$): δ = –14.5 (1 Si^{1}), –5.8 (3 Si^{2}) ppm. IR (KBr): ṽ = 3070, 3047, 2989, 2970, 2907, 2878, 1630 (s, C=C), 1253 (m, CH$_3$ bending), 1132, 820 (s, Si–C), 808 (s, Si–C) cm^{-1}. ESI-TOF: *m*/*z* (%) = 827.23 (100) [M + K]$^{+}$. $C_{45}H_{55}BrSi_4$ (788.16): calcd. C 68.57, H 7.03; found C 68.56, H 7.13.

1-Bromo-4-{tris[4-(triallylsilyl)phenyl]silyl}benzene (8d): The same procedure as in the preparation of **8a** was used to prepare **8d**: *n*BuLi (2.5 M, 22.3 mmol, 8.95 mL, *n*-hexane), **5c** (22.3 mmol, 6.84 g) in diethyl ether (100 mL), TMEDA (33.42 mmol, 3.883 g, 5 mL), and **3d** (7.075 mmol, 2.055 g) in diethyl ether (40 mL). Silica gel column chromatography (*n*-hexane/20% dichloromethane/*n*-hexane; column size: 4 × 35 cm) afforded **8d** (2.350 g, 2.713 mmol, 38%) as a colorless solid. M.p. 69.0 °C. ^{1}H NMR (CDCl$_3$): δ = 7.53 [s, 6 H (H^{6}) + 6 H (H^{7})], 7.53 (dt, *J* = 8.42, 1.82 Hz, 2 H, H^{2}), 7.41 (dt, *J* = 8.42, 1.82 Hz, 2 H, H^{3}), 5.81 (ddt, *J* = 16.93, 10.09, 8.02 Hz, 9 H, H^{10}), 4.94 (ddt, *J* = 16.93, 2.81, 1.16 Hz, 9 H, H^{11}), 4.92 (ddt, *J* = 10.09, 2.81, 1.16 Hz, 9 H, H^{11}), 1.88 (dt, *J* = 8.02, 1.16 Hz, 18 H, H^{9}) ppm. ^{13}C{^{1}H} NMR (CDCl$_3$): δ = 137.9 (2 C^{3}), 137.3 (3 C^{8}), 135.4 (6 C^{6}), 134.5 (3 C^{5}), 133.7 (9 C^{10}), 133.6 (6 C^{7}), 132.9 (1 C^{4}), 131.1 (2 C^{2}), 124.8 (1 C^{1}), 114.4 (9 C^{11}), 19.5 (9 C^{9}) ppm. ^{29}Si{^{1}H} NMR (CDCl$_3$): δ = –14.6 (1 Si^{1}), –8.0 (3 Si^{2}) ppm. IR (KBr): ṽ = 3070, 3047, 2996, 2966, 2908, 2878, 1630 (s, C=C), 1132, 794 (m, Si–C) cm^{-1}. ESI-TOF: *m*/*z* (%) = 905.24 (22) [M + K]$^{+}$. $C_{51}H_{61}BrSi_4$ (866.28): calcd. C 70.71, H 7.10; found C 70.34, H 6.98.

Tris(4-{tris[4-(allyldimethylsilyl)phenyl]silyl}phenyl)silyl Chloride (10a): *t*BuLi (1.7 M, 2.00 mmol, 1.18 mL, *n*-pentane) was added dropwise to **8b** (1.00 mmol, 0.710 g) dissolved in diethyl ether (7 mL) at –76 °C. The reaction solution was stirred at this temperature for 1 h and then diluted with THF (60 mL). SiCl$_4$ dissolved in THF (0.0436 M, 0.30 mmol, 6.9 mL) was added dropwise, and stirring was continued at this temperature for 20 min and then at 25 °C for 24 h. The reaction mixture was treated with water (50 mL) and was then extracted with diethyl ether (100 mL). The organic layer was dried with magnesium sulfate, and all volatiles were removed in an oil-pump vacuum. The crude product was purified by dissolving it in dichloromethane/*n*-pentane of ratio (1:9, 50 mL) and cooling it to –30 °C. Pure **10a** could be isolated as a colorless solid (0.332 g, 0.170 mmol, 57%). M.p. 345 °C (decomp.). ^{1}H NMR (C$_6$D$_6$, 10 mM, 75 °C): δ = 7.72 [m, 6 H (H^{2}) + 6 H (H^{3}) + 18 H (H^{7})], 7.45 (br. d, *J* = 7.50 Hz, 18 H, H^{6}), 5.75 (m, 9 H, H^{10}), 4.87 (m, 9 H, H^{11}), 4.85 (m, 9 H, H^{11}), 1.69 (br. d, *J* = 8.00 Hz, 18 H, H^{9}), 0.21 (s, 54 H, H^{12}) ppm. ^{13}C{^{1}H} NMR (CDCl$_3$): δ = 140.2 (9 C^{8}), 136.4 (3 C^{1}), 136.1 (3 C^{4}) 135.7 (6 C^{3}), 135.5 (18 C^{6}), 134.5 (9 C^{10}), 134.4 (9 C^{5}), 134.2 (6 C^{2}), 132.9 (18 C^{7}), 113.4 (9 C^{11}), 23.5 (9 C^{9}), –3.6 (18 C^{12}) ppm. ^{29}Si{^{1}H} NMR (CDCl$_3$): δ = –14.7 (3 Si^{2}), –12.7 (1 Si^{1}), –4.6 (9 Si^{3}) ppm. IR (KBr): ṽ = 3070, 3050, 2996, 2955, 2908, 1629 (m, C=C), 1250 (m, CH$_3$ bending), 1133, 837 (s, Si–C), 802 (s, Si–C) cm^{-1}. MALDI-TOF MS: calcd. for $C_{124}H_{152}O_4Si_{13}$ 2069.9; found 2069.7. $C_{117}H_{147}ClSi_{13}$ (1953.98): calcd. C 71.92, H 7.58; found C 71.68, H 7.49.

Tris[4-(tris{4-[diallyl(methyl)silyl]phenyl}silyl)phenyl]silyl Chloride (10b): The same procedure as discussed for the synthesis of **10a** was used in the preparation of **10b**: *t*BuLi (1.7 M, 6.00 mmol, 3.53 mL, *n*-pentane), **8c** (3.00 mmol, 2.361 g) in diethyl ether (20 mL), THF (170 mL), and SiCl$_4$ in THF (0.0436 M, 0.75 mmol, 17.2 mL). The obtained product was purified by dissolving it in a mixture of dichloromethane/*n*-pentane in a ratio of 1:9 (100 mL) to give on cooling to –30 °C pure **10b** (0.808 g, 0.3690 mmol, 49%) as a colorless solid. M.p. 340 °C (decomp). ^{1}H NMR (C$_6$D$_6$, 9.5 mM, 75 °C): δ = 7.72 [m, 6 H (H^{2}) + 6 H (H^{3}) + 18 H (H^{7})], 7.47 (m, 18 H, H^{6}), 5.75 (ddt, *J* = 17.32, 9.69, 7.83 Hz, 18 H, H^{10}), 4.88 (ddt, *J* = 17.32, 2.25, 1.13 Hz, 18 H, H^{11}), 4.85 (ddt, *J* = 9.69, 2.25, 1.13 Hz, 18 H, H^{11}), 1.74 (dt, *J* = 7.83, 1.13 Hz, 18 H, H^{9}), 0.23 (s, 27 H, H^{12}) ppm. ^{13}C{^{1}H} NMR (CDCl$_3$): δ = 138.6 (9 C^{8}), 136.4 (3 C^{1}), 136.2 (3 C^{4}), 135.7 (6 C^{3}), 135.5 (18 C^{6}), 134.6 (9 C^{5}), 134.2 (6 C^{2}), 134.1 (18 C^{10}), 133.3 (18 C^{7}), 113.7 (18 C^{11}), 21.5 (18 C^{9}), –5.9 (9 C^{12}) ppm. ^{29}Si{^{1}H} NMR (CDCl$_3$): δ = –14.7 (3 Si^{2}), –12.8 (1 Si^{1}), –5.8 (9 Si^{3}) ppm. IR (KBr): ṽ = 3070, 3052, 2996, 2967, 2908, 2878, 1630 (m, C=C), 1252 (m, CH$_3$ bending), 1133, 820 (s, Si–C), 805 (s, Si–C) cm^{-1}. $C_{135}H_{165}ClSi_{13}$ (2188.32): calcd. C 74.10, H 7.60; found C 73.96, H 7.51.

Tetrakis(4-{tris[4-(allyldimethylsilyl)phenyl]silyl}phenyl)silane (11a): *t*BuLi (1.7 M, 16.2 mmol, 9.53 mL, *n*-pentane) was added dropwise to **8b** (8.1 mmol, 5.75 g) dissolved in diethyl ether (40 mL) at –76 °C. The reaction solution was stirred at this temperature for 1 h, then TMEDA (8.5 mmol, 1.0 g, 1.3 mL) was added in a single portion, and stirring was continued for 5 min. SiCl$_4$ (2.0 mmol, 0.34 g, 0.23 mL) dissolved in THF (120 mL) was added dropwise, and stirring was continued at –20 °C for 20 min and at 25 °C for 24 h. The reaction mixture was then treated with water (100 mL), and the resulting mixture was extracted with diethyl ether (150 mL). The organic layer was dried with magnesium sulfate, and all volatile materials were removed in an oil-pump vacuum. The crude product was purified by silica gel column chromatography (*n*-hexane/20% dichloromethane/*n*-hexane; column size: 4 × 45 cm) to give **11a** (2.1 g, 0.824 mmol, 41%) as a colorless solid. M.p. 380 °C (decomp.). ^{1}H NMR (C$_6$D$_6$, 75 °C, 7.8 mM): δ = 7.90–7.18 [m, 8 H (H^{2}) + 8 H (H^{3}) + 24 H (H^{6}) + 24 H (H^{7})], 5.74 (m, 12 H, H^{10}), 4.86 (br. d, *J* = 17.00 Hz, 12 H, H^{11}), 4.85 (br. d, *J* = 10.00 Hz, 12 H, H^{11}), 1.69 (br. d, *J* = 7.75 Hz, 24 H, H^{9}), 0.21 (br. s, 72 H, H^{12}) ppm. ^{13}C{^{1}H} NMR (CDCl$_3$, 21.6 mM, 25 °C): δ = 140.3 (C^{8}), 140.2 (C^{8}), 139.6 (12 C^{5}), 135.6 (C^{6}), 135.5 (C^{6}), 135.2 (4 C^{4}), 134.7 (4 C^{1}), 134.6 (8 C^{2}), 134.3 (12 C^{10}), 132.9 (C^{7}), 132.8 (C^{7}), 132.7 (8 C^{3}), 113.5 (C^{11}), 113.4 (C^{11}), 23.6 (C^{9}), 23.5 (C^{9}), –3.5 (C^{12}), –3.6 (C^{12}) ppm. ^{29}Si{^{1}H} NMR (C$_6$D$_6$, 75 °C, 10 mM):

δ = –14.3 (br., 1 Si^{1} & 4 Si^{2}), –5.0 (12 Si^{3}) ppm. IR (KBr disc): ṽ = 3070, 3050, 2996, 2955, 2909, 1629 (m, C=C), 1250 (m, CH$_3$ bending), 1132, 836 (m, Si–C), 802 (m, Si–C) cm^{-1}. MALDI-TOF MS: calcd. for $C_{156}H_{196}AgSi_{17}$ 2656.1; found 2655.7. $C_{156}H_{196}Si_{17}$ (2548.68): calcd. C 73.52, H 7.75; found C 73.83, H 7.80.

Tetrakis[4-(tris{4-[diallyl(methyl)silyl]phenyl}silyl)phenyl]silane (11b): *t*BuLi (1.7 M, 2.64 mmol, 1.55 mL, *n*-pentane) was added dropwise to **8c** (1.32 mmol, 1.040 g) dissolved in diethyl ether (7 mL) at –76 °C. The reaction solution was stirred at this temperature for 1 h, then TMEDA (1.98 mmol, 0.230 g, 0.30 mL) was added in a single portion, and stirring was continued for 5 min. The resulting reaction mixture was diluted with THF (15 mL), afterwards $SiCl_4$ in THF (43.6 mM, 0.30 mmol, 6.88 mL) was added, and stirring was continued at this temperature for 20 min and at 25 °C for 24 h. The reaction mixture was quenched with water (50 mL) and was then extracted with diethyl ether (100 mL). The organic layer was dried with magnesium sulfate, and all volatiles were removed in an oil-pump vacuum. The crude product was purified by column chromatography (*n*-hexane/20% dichloromethane/*n*-hexane; column size: 4 × 25 cm) to give **11b** (0.173 g, 0.061 mmol, 20%) as a colorless solid. M.p. 375 °C (decomp.). ^{1}H NMR (C_6D_6, 75 °C, 3.8 mM): δ = 7.73 [m, 8 H (H^{2}) + 8 H (H^{3})], 7.71 (br. d, *J* = 7.63 Hz, 24 H, H^{7}), 7.45 (br. d, *J* = 7.63 Hz, 24 H, H^{6}), 5.75 (m, 24 H, H^{10}), 4.88 (br. d, *J* = 17.63 Hz, 24 H, H^{11}), 4.86 (br. d, *J* = 9.63 Hz, 24 H, H^{11}), 1.74 (br. d, *J* = 8.00 Hz, 48 H, H^{9}), 0.23 (br. s, 36 H, H^{12}) ppm. ^{13}C{^{1}H} NMR ($CDCl_3$, 19.2 mM): δ = 138.6 (12 C^{8}), 138.2 (12 C^{5}), 135.6 (C^{6}), 135.5 (C^{6}), 134.7 (4 C^{4}), 134.4 (4 C^{1}), 134.1 (24 C^{10}),133.8 (8 C^{2}), 133.3 (C^{7}), 133.2 (C^{7}), 133.1 (8 C^{3}), 114.0 (C^{11}), 113.9 (C^{11}), 21.5 (24 C^{9}), –5.8 (C^{12}), –5.9 (C^{12}) ppm. ^{29}Si{^{1}H} NMR (C_6D_6, 75 °C, 8.7 mM): δ = –14.4 (br., 1 Si^{1} and 4 Si^{2}), –6.0 (12 Si^{3}) ppm. IR (KBr): ṽ = 3070, 3052, 2996, 2967, 2915, 2878, 1630 (m, C=C), 1252 (m, CH$_3$ bending), 1132, 817 (s, Si–C), 806 (s, Si–C) cm^{-1}. $C_{180}H_{220}Si_{17}$ (2861.13): calcd. C 75.56, H 7.75; found C 75.20, H 8.02.

1-Bromo-4-[tris(4-{tris[4-(allyldimethylsilyl)phenyl]silyl}phenyl)silyl]benzene (12b): *t*BuLi (1.7 M, 6.866 mmol, 4.04 mL, *n*-pentane) was added dropwise to **8b** (3.433 mmol, 2.44 g) in diethyl ether (25 mL) at –76 °C. The reaction mixture was stirred at this temperature for 1 h. Compound **3d** (1.133 mmol, 0.33 g) dissolved in THF (85 mL) was then added dropwise, and stirring was continued at –20 °C for 20 min and then at 25 °C for 24 h. The reaction mixture was afterwards treated with water (50 mL), and the resulting mixture was extracted with diethyl ether (100 mL). The organic layer was dried with magnesium sulfate, and all volatile materials were removed in an oil-pump vacuum. The crude product was purified by silica gel column chromatography (*n*-hexane/20% dichloromethane/*n*-hexane; column size: 4 × 25 cm) to give **12b** (0.545 g, 0.263 mmol, 23%) as a colorless solid. M.p. 360 °C (decomp.). ^{1}H NMR (C_6D_6, 12 mM, 75 °C): δ = 7.75 (br. d, *J* = 7.64 Hz, 6 H, H^{7}), 7.72 (br. d, *J* = 7.36 Hz, 18 H, H^{11}), 7.67 (br. d, *J* = 7.64 Hz, 6 H, H^{6}), 7.45 (br. d, *J* = 7.36 Hz, 18 H, H^{10}), 7.37 (br. d, *J* = 7.78 Hz, 2 H, H^{2}), 7.25 (br. d, *J* = 7.78 Hz, 2 H, H^{2}), 5.75 (ddt, *J* = 16.66, 10.25, 7.99 Hz, 9 H, H^{14}), 4.86 (br. d, *J* = 16.66 Hz, 9 H, H^{15}), 4.85 (br. d, *J* = 10.25 Hz, 9 H, H^{15}), 1.69 (br. d, *J* = 7.99 Hz, 18 H, H^{13}), 0.31 (s, 54 H, H^{16}) ppm. ^{13}C{^{1}H} NMR ($CDCl_3$, 30 mM, 25 °C): δ = 140.3 (C^{12}), 139.7 (C^{12}), 138.0 (2 C^{3}), 136.0 (3 C^{8}), 135.7 (6 C^{6}), 135.5 (18 C^{10}), 135.3 (C^{4}), 134.6 (C^{9}), 134.5 (9 C^{14}), 134.4 (C^{9}), 134.3 (C^{9}), 134.2 (C^{5}), 134.0 (C^{5}), 132.9 (18 C^{11}), 132.7 (6 C^{7}), 131.1 (2 C^{2}), 124.8 (1 C^{1}), 113.4 (9 C^{15}), 23.5 (9 C^{13}), –3.6 (18 C^{16}) ppm. ^{29}Si{^{1}H} NMR (C_6D_6, 30 mM, 25 °C): δ = –14.0 (3 Si^{2}), –13.7 (1 Si^{1}), –4.9 (9 Si^{3}) ppm. IR (KBr): ṽ = 3070, 3050, 2996, 2956, 2908, 2885, 1629 (m, C=C), 1250 (m, CH$_3$ bending), 1133, 836 (s, Si–C), 802 (s, Si–C) cm^{-1}. MALDI-TOF MS: *m*/*z* calcd. for $C_{123}H_{151}AgBrSi_{13}$ 2181.7; found 2181.9. $C_{123}H_{151}BrSi_{13}$ (2074.53): calcd. C 71.21, H 7.34; found C 70.94, H 7.24.

1-Bromo-4-{tris[4-(tris{4-[diallyl(methyl)silyl]phenyl}silyl)phenyl]silyl}benzene (12c): The same procedure as discussed for the preparation of **12b** was used in the synthesis of **12c**: *t*BuLi (1.7 M, 7.134 mmol, 4.2 mL, *n*-pentane), **8c** (3.567 mmol, 2.81 g) in diethyl ether (25 mL), and **3d** (1.133 mmol, 0.33 g) in THF (85 mL). Silica gel column chromatography (*n*-hexane/20% dichloromethane/*n*-hexane; column size: 4 × 25 cm) afforded **12c** (0.69 g, 0.3 mmol, 26%) as a colorless solid. M.p. 355 °C (decomp.). ^{1}H NMR (C_6D_6, 12 mM, 75 °C): δ = 7.73 (br. d, *J* = 7.52 Hz, 6 H, H^{7}), 7.72 (br. d, *J* = 7.90 Hz, 18 H, H^{11}), 7.66 (br. d, *J* = 7.52 Hz, 6 H, H^{6}), 7.46 (br. d, *J* = 7.90 Hz, 18 H, H^{10}), 7.35 (br. d, *J* = 8.22 Hz, 2 H, H^{2}), 7.24 (br. d, *J* = 8.22 Hz, 2 H, H^{3}), 5.74 (ddt, *J* = 16.91, 10.12, 7.94 Hz, 18 H, H^{14}), 4.87 (ddt, *J* = 16.91, 1.95, 1.10 Hz, 18 H, H^{15}), 4.85 (ddt, *J* = 10.12, 1.95, 1.10 Hz, 18 H, H^{15}), 1.74 (dt, *J* = 7.95, 1.10 Hz, 18 H, H^{13}), 0.23 (s, 27 H, H^{16}) ppm. ^{13}C{^{1}H} NMR ($CDCl_3$, 22 mM, 25 °C): δ = 138.6 (9 C^{12}), 138.3 (3 C^{8}), 138.0 (2 C^{3}), 136.9 (1 C^{4}), 135.7 (6 C^{6}), 135.6 (C^{10}), 135.5 (C^{10}), 134.6 (9 C^{9}), 134.3 (3 C^{5}), 134.1 (18 C^{14}), 133.8 (6 C^{7}), 133.3 (C^{11}), 133.1 (C^{11}), 131.1 (2 C^{2}), 124.9 (C^{1}), 124.8 (C^{1}), 114.0 (C^{15}), 113.9 (C^{15}), 21.5 (18 C^{13}), –5.7 (C^{16}), –5.9 (C^{16}) ppm. ^{29}Si{^{1}H} NMR ($CDCl_3$, 55 °C): δ = –14.8 (3 Si^{2}), –13.4 (1 Si^{1}), –5.9 (9 Si^{3}) ppm. IR (KBr): ṽ = 3070, 3051, 2996, 2967, 2908, 2878, 1630 (m, C=C), 1252 (m, CH$_3$ bending), 1133, 820 (s, Si–C), 805 (s, Si–C) cm^{-1}. $C_{141}H_{169}BrSi_{13}$ (2308.87): calcd. C 73.35, H 7.38; found C 72.93, H 7.33.

1-Bromo-4-[tris(4-{tris-[4-(triallylsilyl)phenyl]silyl}phenyl)silyl]benzene (12d): The same procedure as applied in the synthesis of **12b** was used in the preparation of **12d**: *t*BuLi (1.7 M, 3.96 mmol, 2.33 mL, *n*-pentane), **8d** (1.982 mmol, 1.71 g) in diethyl ether (20 mL), and **3d** (0.654 mmol, 0.190 g) in THF (60 mL). Silica gel column chromatography (*n*-hexane/20% dichloromethane/*n*-hexane; column size: 2 × 25 cm) to give **12d** (0.140 g, 0.0550 mmol, 8.4%) as a colorless solid. M.p. 350 °C (decomp.). ^{1}H NMR (C_6D_6, 55 °C, 10 mM): δ = 7.73 (br. d, *J* = 8.0 Hz, 18 H, H^{11}), 7.72 (br. d, *J* = 7.81 Hz, 6 H, H^{7}), 7.62 (br. d, *J* = 7.81 Hz, 6 H, H^{6}), 7.48 (br. d, *J* = 8.0 Hz, 18 H, H^{10}), 7.32 (br. d, *J* = 8.38 Hz, 2 H, H^{2}), 7.22 (br. d, *J* = 8.38 Hz, 2 H, H^{3}), 5.76 (ddt, *J* = 16.92, 10.07, 7.98 Hz, 27 H, H^{14}), 4.91 (ddt, *J* = 16.92, 2.02, 1.16 Hz, 27 H, H^{15}), 4.87 (ddt, *J* = 10.07, 2.02, 1.16 Hz, 27 H, H^{15}), 1.79 (dt, *J* = 7.98, 1.16 Hz, 54 H, H^{13}) ppm. ^{13}C{^{1}H} NMR ($CDCl_3$, 25 °C, 30 mM): δ = 138.0 (2 C^{3}), 137.1 (9 C^{12}), 135.8 (6 C^{6}), 135.6 (6 C^{7}), 135.5 (18 C^{10}), 134.8 (9 C^{9}), 134.4 (3 C^{8}), 133.7 (27 C^{14}), 133.6 (18 C^{11}), 132.9 (1 C^{4}), 132.7 (3 C^{5}), 131.1 (2 C^{2}), 124.9 (1 C^{1}), 114.4 (27 C^{15}), 19.5 (27 C^{13}) ppm. ^{29}Si{^{1}H} NMR ($CDCl_3$, 50 °C, 20 mM): δ = –14.7 (3 Si^{2}), –14.3 (1 Si^{1}), –8.0 (9 Si^{3}) ppm. IR (KBr): ṽ = 3070, 3048, 2996, 2967, 2915, 2878, 1630 (m, C=C), 1133, 798.2 (m, Si–C) cm^{-1}. $C_{157}H_{187}BrSi_{13}$ (2543.20): calcd. C 75.09, H 7.41; found C 75.24, H 7.13.

Crystal Structure Determination: Crystal data for **7b** and **10a** are presented in Table S1 (Supporting Information). The data for **7b** were collected with a Bruker Smart CCD 1k diffractometer at 183 K and those of **10a** with a Stoe IPDS-II/2T diffractometer, both with graphite-monochromated Mo-K_{α} (λ = 0.71073 Å) radiation. The structures were solved by direct methods using SHELXS-97[30] and refined by full-matrix least-squares procedures on F^2 using SHELXL-97.[31] All non-hydrogen atoms were refined anisotropically, and a riding model was employed in the refinement of the hydrogen-atom positions. In the case of **7b**, the atoms C21/C22, C32/C33, C54/C55, C87/C88, C109/C110, and C95/C96/C98/C99 were refined disordered on two positions with occupation factors of 0.71, 0.53, 0.70, 0.51, 0.70, and 0.66, respectively. In the case of **10a**, the asymmetric unit comprises an *n*-pentane molecule with an occupation factor of 0.5. The occupation factor was fixed after pre-refinements gave values close to 0.5. The atoms C115–C117 were refined disordered on two positions with an occupation factor of 0.47. During the measurements, although performed at 100 K, a significant decrease in the intensities of the standard reflections was observed. Together with this effect, a number of additional reflections appeared that did not belong to the unit cell mentioned here. The same effect was observed when measuring other crystals. It was thus concluded that the specific compound and/or its crystals do show a phase transition at approximately 100 K or that the *n*-pentane as packing solvent "evaporates" slowly, but thereby permanently destroying the single-crystal property. The measurement was thus optimized in the sense that the largest suitable crystal was selected, and exposure times were set to minimum requirements. Despite this, the completeness reached only 87% to θ = 24.4°. CCDC-905944 (**7b**) and -905943 (**10a**) contain the supplementary crystallographic data for this paper. These data can be obtained free of charge from The Cambridge Crystallographic Data Centre via www.ccdc.cam.ac.uk/data_request/cif.

Supporting Information (see footnote on the first page of this article): Atom numbering scheme, crystal data and structure refinemnt parameters, tables concerning hydrogen bonding interactions.

Acknowledgments

We gratefully acknowledge generous financial support from the Deutsche Forschungsgemeinschaft and the Fonds der Chemischen Industrie.

---

[1] a) D. Astruc, E. Boisselier, C. Ornelas, *Chem. Rev.* **2010**, *110*, 1857; b) G. R. Newkome, C. N. Moorefield, F. Vögtle, *Dendritic Molecules – Concepts, Syntheses, Perspectives*, VCH, Weinheim, **1996**; c) B. I. Voit, *Acta Polym.* **1995**, *46*, 87; d) N. Ardoin, D. Astruc, *Bull. Soc. Chim. Fr.* **1995**, *132*, 875; e) J. Issberner, R. Moors, F. Vögtle, *Angew. Chem.* **1994**, *106*, 2507; *Angew. Chem. Int. Ed. Engl.* **1994**, *33*, 2413; f) D. A. Tomalia, A. M. Naylor, W. A. Goddart, *Angew. Chem.* **1990**, *102*, 119; *Angew. Chem. Int. Ed. Engl.* **1990**, *29*, 138; g) D. A. Tomalia, *Aldrichim. Acta* **1993**, *26*, 91; h) D. A. Tomalia, H. D. Durst, *Top. Curr. Chem.* **1993**, *165*, 193; i) J. S. Moore, *Polym. News* **1993**, *18*, 5.

[2] a) A. Archut, F. Vögtle, *Chem. Soc. Rev.* **1998**, *27*, 233; b) A. Archut, J. Issberner, F. Vögtle, *Organic Synthesis Highlights III*, Wiley-VCH, Weinheim, **1998**, p. 391; c) A. W. Bosman, H. M. Jansssen, E. W. Meijer, *Chem. Rev.* **1999**, *99*, 1665; d) G. R. Newkome, E. He, C. N. Moorefield, *Chem. Rev.* **1999**, *99*, 1689; e) A. Sekiguchi, V. Y. Lee, M. Nanjo, *Coord. Chem. Rev.* **2000**, *210*, 11; f) M. Fischer, F. Vögtle, *Angew. Chem.* **1999**, *111*, 934; *Angew. Chem. Int. Ed.* **1999**, *38*, 884.

[3] a) X. Peng, Q. Pan, G. L. Rempel, *Chem. Soc. Rev.* **2008**, *37*, 1619; b) K. Fujita, T. Muraki, H. Hattori, T. Sakakura, *Tetrahedron Lett.* **2006**, *47*, 4831; c) J. W. Kriesel, T. D. Tilley, *Chem. Mater.* **2000**, *12*, 1171; d) N. J. Hovestad, E. B. Eggeling, H. J. Heidbüchel, J. T. B. H. Jastrzebski, U. Kragl, W. Keim, D. Vogt, G. van Koten, *Angew. Chem.* **1999**, *111*, 1763; *Angew. Chem. Int. Ed.* **1999**, *38*, 1655; e) J. W. Kriesel, T. D. Tilley, *Adv. Mater.* **2001**, *13*, 1645; f) G. Rodríguez, M. Lutz, A. L. Spek, G. van Koten, *Chem. Eur. J.* **2002**, *8*, 46; g) A. W. Kleij, R. A. Gossage, J. M. K. Gebbink, N. Brinkmann, E. J. Reijerse, U. Kragl, M. Lutz, A. L. Spek, G. van Koten, *J. Am. Chem. Soc.* **2000**, *122*, 12112; h) E. B. Eggeling, N. J. Hovestad, J. T. B. H. Jastrzebski, D. Vogt, G. van Koten, *J. Org. Chem.* **2000**, *65*, 8857; i) G. E. Oosterom, S. Steffens, J. N. H. Reek, P. C. J. Kamer, P. W. N. M. van Leeuwen, *Top. Catal.* **2002**, *19*, 61; j) A. W. Kleij, R. J. M. K. Gebbink, P. A. J. van den Nieuwenhuijzen, H. Kooijman, M. Lutz, A. L. Spek, G. van Koten, *Organometallics* **2001**, *20*, 647; k) R. Roesler, B. J. N. Har, W. E. Piets, *Organometallics* **2002**, *21*, 4300; l) D. de Groot, E. B. Eggeling, J. C. de Wilde, H. Kooijman, R. J. van Haaren, A. W. van der Made, A. L. Spek, D. Vogt, J. N. H. Reek, P. C. J. Kamer, P. W. N. M. van Leeuwen, *Chem. Commun.* **1999**, 1623; m) B. Helms, J. M. Fréchet, *Adv. Synth. Catal.* **2006**, *348*, 1125; n) D. Astruc, F. Chardac, *Chem. Rev.* **2001**, *101*, 2991.

[4] a) B. Donnio, S. Buathong, I. Bury, D. Guillon, *Chem. Soc. Rev.* **2007**, *36*, 1495; b) R. M. Richardson, S. A. Ponomarenko, N. I. Boiko, V. P. Shibaev, *Liq. Cryst.* **1999**, *26*, 101; c) N. Boiko, X. Zhu, A. Bobrovsky, V. Shibaev, *Chem. Mater.* **2001**, *13*, 1447; d) M. R. Wilson, J. M. Ilnytskyi, L. M. Stimson, *J. Chem. Phys.* **2003**, *119*, 3509; e) G. Dantlgraber, U. Baumeister, S. Diele, H. Kresse, B. Lühmann, H. Lang, C. Taschierske, *J. Am. Chem. Soc.* **2002**, *124*, 1485; f) A. Y. Bobrovsky, A. A. Pakhomov, X.-M. Zhu, N. I. Boiko, V. P. Shibaev, J. Stumpe, *J. Phys. Chem. B* **2002**, *106*, 540; g) S. A. Ponomarenko, N. I. Boiko, V. P. Shibaev, S. N. Magonov, *Langmuir* **2000**, *16*, 5487; h) N. I. Boiko, A. I. Lysachkov, S. A. Ponomarenko, V. P. Shibaev, R. M. Richardson, *Colloid Polym. Sci.* **2005**, *283*, 1155; i) S. A. Ponomarenko, N. I. Boiko, V. P. Shibaev, R. M. Richardson, I. J. Whitehouse, E. A. Rebrov, A. M. Muzafarov, *Macromolecules* **2000**, *33*, 5549; j) K. L. Genson, J. Holzmueller, I. Leshchiner, E. Agina, N. Boiko, V. P. Shibaev, V. V. Tsukruk, *Macromolecules* **2005**, *38*, 8028; k) M. Marcos, R. Martin-Rapún, A. Omenat, J. L. Serrano, *Chem. Soc. Rev.* **2007**, *36*, 1889.

[5] a) A. Agarwal, A. Asthana, U. Gupta, N. K. Jain, *J. Pharm. Pharmacol.* **2008**, *60*, 671; b) Y. Cheng, J. Wang, T. Rao, X. He, T. Xu, *Front. Biosci.* **2008**, *13*, 1447; c) Y. Cheng, Z. Xu, M. Ma, T. Xu, *J. Pharm. Sci.* **2008**, *97*, 123; d) H. L. Crampton, E. E. Simanek, *Polym. Int.* **2007**, *56*, 489; e) K. Nishikawa, K. Matsuoka, E. Kita, N. Okabe, M. Mizuguchi, K. Hino, S. Miyazawa, C. Yamasaki, J. Aoki, S. Takashima, Y. Yamakawa, M. Nishijima, D. Terunuma, H. Kuzuhara, Y. Natori, *Proc. Natl. Acad. Sci. USA* **2002**, *99*, 7669; f) R. Esfand, D. A. Tomalia, *Drug Discovery Today* **2001**, *6*, 427.

[6] a) A. Trinchi, T. H. Muster, *Supramol. Chem.* **2007**, *19*, 431; b) R. Buschbeck, S. Mecklenburg, B. Lühmann, V. K. Gupta, H. Lang, *Synthesis* **2004**, 2727; c) R. Buschbeck, H. Lang, S. Agarwal, V. K. Saini, V. K. Gupta, *Synthesis* **2004**, 1243; d) P. Lhotak, S. Shinkai, *Tetrahedron* **1995**, *51*, 7681.

[7] a) P. R. Dvornic, J. Li, A. M. deLeuze-Jallouli, S. D. Reeves, M. J. Owen, *Macromolecules* **2002**, *35*, 9323; b) H. Ma, A. K.-Y. Jen, *Adv. Mater.* **2001**, *13*, 1201; c) S. Dietrich, S. Schulze, M. Hietschold, H. Lang, *J. Colloid Interface Sci.* **2011**, *359*, 454.

[8] R. M. Laine, M. F. Roll, *Macromolecules* **2011**, *44*, 1073.

[9] a) H. Schumann, Y. Aksu, S. Schutte, B. C. Wassermann, S. H. Müehle, *J. Organomet. Chem.* **2006**, *691*, 4717; b) R. Meijboom, M. J. Overett, J. R. Moss, *J. Organomet. Chem.* **2004**, *689*, 987; c) S. Arévalo, J. M. Benito, E. de Jesús, F. J. de la Mata, J. C. Flores, R. Gómez, *J. Organomet. Chem.* **2000**, *602*, 208; d) K. Brüning, H. Lang, *J. Organomet. Chem.* **1998**, *571*, 145; e) J. W. J. Knapen, A. W. van der Made, J. C. de Wilde, P. W. N. M. van Leeuwen, P. Wijkens, D. M. Grove, G. van Koten, *Nature* **1994**, *372*, 659; f) M. Zamora, B. Alonso, C. Pastor, I. Cuadrado, *Organometallics* **2007**, *26*, 5153; g) R. Andrés, E. de Jesús, F. J. de la Mata, J. C. Flores, R. Gómez, *Eur. J. Inorg. Chem.* **2002**, *9*, 2281; h) A. W. van der Made, P. W. N. M. van Leeuwen, J. C. de Wilde, R. A. C. Brandes, *Adv. Mater.* **1993**, *5*, 466; i) J. Le Nôtre, J. J. Firet, L. A. J. M. Sliedregt, B. J. Van Steen, G. Van Koten, J. M. K. Robertus, *Org. Lett.* **2005**, *7*, 363.

[10] a) R. Gras, M. Relloso, M. I. García, F. J. de la Mata, R. Gómez, L. A. López-Fernández, M. A. Muñoz-Fernández, *Biomaterials* **2012**, *33*, 4002; b) B. Rasines, J. Sánchez-Nieves, I. T. Molina, M. Guzmán, M. A. Munõz-Fernández, R. Gómez, F. J. de la Mata, *New J. Chem.* **2012**, *36*, 360; c) E.

Arnáiz, L. I. Doucede, S. García-Gallego, K. Urbiola, R. Gómez, C. Tros de Ilarduya, F. J. de la Mata, *Mol. Pharmaceutics* **2012**, *9*, 433; d) I. Angurell, L. I. Rodríguez, O. Rossell, M. Seco, *Organometallics* **2011**, *30*, 5771; e) D. Seyferth, T. Kugita, A. L. Rheingold, G. P. A. Yap, *Organometallics* **1995**, *14*, 5362; f) C. Kim, M. Kim, *J. Organomet. Chem.* **1998**, *563*, 43; g) M. Zhou, J. Roovers, *Macromolecules* **2001**, *34*, 244; h) B. Rasines, J. M. Hernández-Ros, N. de las Cuevas, J. L. Copa-Patiño, J. Soliveri, M. A. Muñoz-Fernández, R. Gómez, F. J. de la Mata, *Dalton Trans.* **2009**, 8704; i) C. Kim, S. Kang, *J. Polym. Sci., Part A* **2000**, *38*, 724; j) S. Chandra, H. Lang, *Mater. Chem. Phys.* **2009**, *114*, 926; k) S. Chandra, R. Buschbeck, H. Lang, *Talanta* **2006**, *70*, 1087; l) S. Chandra, R. Buschbeck, H. Lang, *Anal. Sci.* **2006**, *22*, 1327; m) H. Hahn, C. Keith, H. Lang, R. A. Reddy, C. Tschierske, *Adv. Mater.* **2006**, *18*, 2629; n) R. Buschbeck, H. Lang, S. Agarwal, V. K. Saini, V. K. Gupta, *Synthesis* **2004**, *8*, 1243; o) G. Dantlgraber, U. Baumeister, S. Diele, H. Kresse, B. Lühmann, H. Lang, C. Tschierske, *J. Am. Chem. Soc.* **2002**, *124*, 14852; p) M. Wander, P. J. C. Hausoul, L. A. J. M. Sliedregt, B. J. van Steen, G. van Koten, R. J. M. Klein Gebbink, *Organometallics* **2009**, *28*, 4406; q) N. J. Hovestad, A. Ford, J. T. B. H. Jastrzebski, G. van Koten, *J. Org. Chem.* **2000**, *65*, 6338.

[11] a) Y. Niu, H. Lu, D. Wang, Y. Yue, S. Feng, *J. Organomet. Chem.* **2012**, *696*, 544; b) C. Kim, H. Kim, *J. Organomet. Chem.* **2003**, *673*, 77; c) E. Lukevics, P. Arsenyan, O. Pudova, *Main Group Met. Chem.* **2002**, *25*, 135; d) A. Morikawa, M. Kakimoto, Y. Imai, *Macromolecules* **1992**, *25*, 3247; e) K. Kawahara, Y. Hagiwara, K. Kuroda, *Chem. Eur. J.* **2011**, *17*, 13188; f) X. Peng, Q. Pan, X. Lu, *J. Appl. Polym. Sci.* **2011**, *122*, 334; g) R. Djeda, A. Rapakousiou, L. Liang, N. Guidolin, J. Ruiz, D. Astruc, *Angew. Chem.* **2010**, *122*, 8328; *Angew. Chem. Int. Ed.* **2010**, *49*, 8152; h) M. Deluge, C. Cai, *Langmuir* **2005**, *21*, 1917.

[12] a) R. Buschbeck, H. Lang, *J. Organomet. Chem.* **2005**, *690*, 1198; b) R. Buschbeck, K. Brüning, H. Lang, *Synthesis* **2001**, *15*, 2289; c) K. Brüning, H. Lang, *Synthesis* **1999**, 1931; d) H. Lang, B. Lühmann, *Adv. Mater.* **2001**, *13*, 1523; e) B. Lühmann, H. Lang, K. Brüning, *Phosphorus, Sulfur Silicon Relat. Elem.* **2001**, *168–169*, 481; f) H. Lang, B. Lühmann, *Phosphorus, Sulfur Silicon Relat. Elem.* **2001**, *168–169*, 297; g) M. L. Zheng, W. Q. Chen, C. F. Li, X. Z. Dong, X. M. Duan, *ChemPhysChem* **2007**, *8*, 810; h) V. K. Gupta, S. Chandra, S. Agarwal, H. Lang, *Sens. Actuators, B* **2005**, *107*, 762; i) H. Namazi, S. Jafarirad, *Int. J. Pharm.* **2011**, *407*, 167; j) C. Kim, H. Kim, *J. Polym. Sci., Part A* **2002**, *40*, 326.

[13] a) M. W. P. L. Baars, R. Kleppinger, M. H. J. Koch, S. L. Yeu, E. W. Meijer, *Angew. Chem.* **2000**, *112*, 1341; *Angew. Chem. Int. Ed.* **2000**, *39*, 1285; b) A. Jawor, E. M. V. Hoek, *Environ. Sci. Technol.* **2010**, *44*, 2570; c) M. S. Diallo, W. Arasho, J. H. Johnson, W. A. Goddard, *Environ. Sci. Technol.* **2008**, *42*, 1572; d) T. Kouketsu, S. Duan, T. Kai, S. Kazama, K. Yamada, *J. Membr. Sci.* **2007**, *287*, 51; e) L. Li, B. Wang, H. Tan, T. Chen, J. J. Xu, *J. Membr. Sci.* **2006**, *269*, 84.

[14] a) K. Itami, K. Terakawa, J.-I. Yoshida, O. Kajimoto, *J. Am. Chem. Soc.* **2003**, *125*, 6058; b) J.-I. Yoshida, K. Muraki, H. Funahashi, N. Kawabata, *J. Org. Chem.* **1986**, *51*, 3996; c) B.-H. Ye, Y. Naruta, *Tetrahedron* **2003**, *59*, 3593; d) F. Moerlein, *J. Organomet. Chem.* **1987**, *319*, 29; e) C. A. Burkhard, *J. Am. Chem. Soc.* **1946**, *68*, 2103.

[15] G. Mignani, M. Barzoukas, J. Zyss, G. Soula, F. Balegroune, D. Grandjean, D. Josse, *Organometallics* **1991**, *10*, 3660.

[16] V. Chvalovskŷ, V. Bažant, *Collect. Czech. Chem. Commun.* **1951**, *16*, 580.

[17] a) Y. Lee, R. B. Silverman, *Tetrahedron* **2001**, *57*, 5339; b) Y. Lee, R. B. Silverman, *Org. Lett.* **2000**, *2*, 303; c) Y. Lee, R. B. Silverman, *Org. Lett.* **2000**, *2*, 3748; d) C. J. Murphy, H. W. Post, *J. Org. Chem.* **1962**, *27*, 1486.

[18] a) X. Deng, A. Mayeux, C. Cai, *J. Org. Chem.* **2002**, *67*, 5279; b) C. M. Yam, J. Cho, C. Cai, *Langmuir* **2004**, *20*, 1228; c) C. M. Yam, J. Cho, C. Cai, *Langmuir* **2003**, *19*, 6862; d) X. Deng, C. Cai, *Tetrahedron Lett.* **2003**, *44*, 815.

[19] M. Wander, P. J. C. Hausoul, L. A. J. M. Sliedregt, B. J. van Steen, G. van Koten, R. J. M. Klein Gebbink, *Organometallics* **2009**, *28*, 4406.

[20] R. H. Meen, H. Gilman, *J. Org. Chem.* **1957**, *22*, 564.

[21] J. Hofmans, L. Maeseele, G. Wang, K. Janssens, M. Van Beylen, *Polymer* **2003**, *44*, 4109.

[22] R. Gossage, E. Muñoz-Martinez, H. Frey, A. Burgath, M. Lutz, A. L. Spek, G. van Koten, *Chem. Eur. J.* **1999**, *5*, 2191.

[23] a) M. O. Sinnokrot, E. F. Valeev, C. D. Sherrill, *J. Am. Chem. Soc.* **2002**, *124*, 10887; b) Y. Zhau, D. G. Truhlar, *J. Phys. Chem. A* **2005**, *109*, 4209; c) K. Kobayashi, Y. Asakawa, Y. Kikuchi, H. Toi, Y. Aoyama, *J. Am. Chem. Soc.* **1993**, *115*, 2648; d) Y. Umezawa, S. Tsuboyama, K. Honda, J. Uzawa, M. Nishio, *Bull. Chem. Soc. Jpn.* **1998**, *71*, 1207; e) T. Fujimoto, R. Yanagihara, K. KobaYashi, Y. Aoyama, *Bull. Chem. Soc. Jpn.* **1995**, *68*, 2113.

[24] a) L. C. Zhang, C. Kabuto, M. Kira, *J. Am. Chem. Soc.* **2002**, *121*, 2925; b) J. B. Lambert, C. L. Stern, Y. Zhao, W. C. Tse, C. E. Shawl, K. T. Lentz, L. Kania, *J. Organomet. Chem.* **1998**, *568*, 21.

[25] a) F. F. Awwadi, S. F. Haddad, R. D. Willett, B. Twamley, *Cryst. Growth Des.* **2010**, *10*, 158; b) F. F. Awwadi, R. D. Willett, K. A. Peterson, B. Twamley, *Chem. Eur. J.* **2006**, *12*, 8952; c) E. Bosch, C. L. Barnes, *Cryst. Growth Des.* **2002**, *2*, 299; d) G. Espallargas, L. Brammer, P. Sherwood, *Angew. Chem.* **2006**, *118*, 449; *Angew. Chem. Int. Ed.* **2006**, *45*, 435.

[26] M. J. Frisch, G. W. Trucks, H. B. Schlegel, G. E. Scuseria, M. A. Robb, J. R. Cheeseman, J. A. Jr., Montgomery, T. Vreven, K. N. Kudin, J. C. Burant, J. M. Millam, S. S. Iyengar, J. Tomasi, V. Barone, B. Mennucci, M. Cossi, G. Scalmani, N. Rega, G. A. Petersson, H. Nakatsuji, M. Hada, M. Ehara, K. Toyota, R. Fukuda, J. Hasegawa, M. Ishida, T. Nakajima, Y. Honda, O. Kitao, H. Nakai, M. Klene, X. Li, J. E. Knox, H. P. Hratchian, J. B. Cross, C. Adamo, J. Jaramillo, R. Gomperts, R. E. Stratmann, O. Yazyev, A. J. Austin, R. Cammi, C. Pomelli, J. W. Ochterski, P. Y. Ayala, K. Morokuma, G. A. Voth, P. Salvador, J. J. Dannenberg, V. G. Zakrzewski, S. Dapprich, A. D. Daniels, M. C. Strain, O. Farkas, D. K. Malick, A. D. Rabuck, K. Raghavachari, J. B. Foresman, J. V. Ortiz, Q. Cui, A. G. Baboul, S. Clifford, J. Cioslowski, B. B. Stefanov, G. Liu, A. Liashenko, P. Piskorz, I. Komaromi, R. L. Martin, D. J. Fox, T. Keith, M. A. Al-Laham, C. Y. Peng, A. Nanayakkara, M. Challacombe, P. M. W. Gill, B. Johnson, W. Chen, M. W. Wong, C. Gonzalez, J. A. Pople, *Gaussian 03*, Revision D.01., Gaussian, Inc., Pittsburgh, PA, **2003**.

[27] G. Socrates, *Infrared Characteristic Group Frequencies*, Wiley, Chichester, **1980**, pp. 126–129.

[28] a) S. M. D. Raper, D. J. Gregg, E. R. Schofield, W. R. Browne, *J. Am. Chem. Soc.* **2004**, *126*, 8694; b) A. S. Shetty, J. Zhang, J. S. Moore, *J. Am. Chem. Soc.* **1996**, *118*, 1019.

[29] K. C. K. Swamy, V. Chandrasekhar, J. J. Harland, J. M. Holmes, R. O. Day, R. R. Holmes, *J. Am. Chem. Soc.* **1990**, *112*, 2341.

[30] G. M. Sheldrick, *Acta Crystallogr., Sect. A* **1990**, *46*, 467.

[31] *SHELXL-97, Program for Crystal Structure Refinement*: G. M. Sheldrick, *Acta Crystallogr., Sect. A* **2008**, *64*, 112.

Received: November 26, 2012
Published Online: February 28, 2013